

NASA Technical Paper 1131

**Feasibility Study of Tungsten
as a Diffusion Barrier Between
Nickel-Chromium-Aluminum and
 γ/γ' - δ Eutectic Alloys**

Stanley G. Young and Glenn R. Zellars

JANUARY 1978

NASA

NASA Technical Paper 1131

Feasibility Study of Tungsten
as a Diffusion Barrier Between
Nickel-Chromium-Aluminum and
 $\gamma/\gamma' - \delta$ Eutectic Alloys

Stanley G. Young and Glenn R. Zellars
Lewis Research Center
Cleveland, Ohio



National Aeronautics
and Space Administration

Scientific and Technical
Information Office

1978

FEASIBILITY STUDY OF TUNGSTEN AS A DIFFUSION BARRIER BETWEEN NICKEL-CHROMIUM-ALUMINUM AND $\gamma/\gamma' - \delta$ EUTECTIC ALLOYS

by Stanley G. Young and Glenn R. Zellars

Lewis Research Center

SUMMARY

High-strength, nickel-base eutectic alloys have potential for high-temperature gas turbine applications. To protect turbine parts from oxidation, coatings of the nickel-chromium-aluminum (NiCrAl) type have shown great promise. However, diffusion of metal atoms between the coating and the substrate causes coating deterioration and subsequent loss of protection for the substrate. In this experimental study, a potential barrier material was inserted between a NiCrAl layer and the eutectic alloy substrate. The intent was to determine the feasibility of minimizing the diffusion between the two layers and thereby prolonging the NiCrAl coating protection of the eutectic alloy in high-temperature environments. The material selected to demonstrate the feasibility of a diffusion barrier concept was tungsten (W). The eutectic alloy was the gamma/gamma prime - delta ($\gamma/\gamma' - \delta$) type, which forms Ni_3Nb (i. e., δ) platelets in a gamma/gamma prime (γ/γ') matrix.

Test specimens were hot-pressed diffusion couples consisting of eutectic/NiCrAl/tungsten/eutectic. This test arrangement permitted the direct comparison of the diffusion at the NiCrAl-eutectic interface to the diffusion that occurs at the NiCrAl-tungsten-eutectic interfaces. Tests were run in vacuum for 250 and 500 hours at 1100°C . Baseline conditions of element distribution were established by metallographic and electron-beam microprobe X-ray analysis of the as-bonded test specimen. Completed test specimens were examined, comparisons were made, and conclusions were drawn from the post-test analyses.

These analyses showed that, without a barrier, diffusion of niobium (Nb) out of the δ phase of the $\gamma/\gamma' - \delta$ substrate destroyed the δ phase and that a mixture of γ/γ' and NiCrAl elements was left in its place. Chromium from the NiCrAl diffused deeply into the γ/γ' of the eutectic alloy. The W layer, on the other hand, completely stopped the diffusion of Nb out of the δ phase into the NiCrAl layer. The diffusion of Cr into the eutectic was greatly reduced by the W, but diffusion of W into the NiCrAl and eutectic and void formation were noted.

The δ phase appeared to be impervious to inward diffusion of W, Cr, and Al. Diffusion into the eutectic alloy was reduced by 30 to 80 percent in depth (depending on the elements examined) when the δ was oriented parallel to the NiCrAl rather than perpendicular. These experiments clearly demonstrated that coating-substrate interdiffusion can be significantly inhibited by the use of barrier techniques.

INTRODUCTION

The fuel efficiency of gas turbine engines is significantly improved as the turbine operating temperatures are increased. Higher turbine efficiencies can be achieved by either improved engine design and/or better materials. Design improvements, however, are frequently limited by the high-temperature strength properties and the oxidation/hot-corrosion resistance of the materials.

Recently, increased interest has been shown in high-strength, nickel-base, directional eutectic alloys for potential use for high-temperature gas-turbine components (refs. 1 and 2). Coatings are necessary for the protection of this class of alloys from severe oxidizing environments (ref. 3). Coatings and claddings of the NiCrAl type have shown great promise for oxidation protection of both eutectic and other high-temperature nickel-base superalloys (refs. 3 and 4). These coatings, however, while initially affording excellent protection against oxidation, interdiffuse with the substrates at elevated temperatures. Prolonged diffusion of metal atoms between the coating and the substrate causes coating compositional changes and subsequent loss of protection for the substrate.

Some recent investigations have been partially successful in reducing diffusion by means of some type of "diffusion barrier" (refs. 5 to 8). Investigators have used oxide barriers on refractory fibers (refs. 5 and 6) and on iron (ref. 7) and metallic barriers on dispersion-strengthened alloys (refs. 8 and 9). The authors of this paper believe that the inclusion of a barrier between the NiCrAl coating and the eutectic alloy substrate may delay or minimize interdiffusion and thereby prolong coating protection in high-temperature environments.

The material selected to demonstrate the feasibility of a diffusion barrier was tungsten. This selection was based on a preliminary survey by the authors. Tungsten, platinum, silicon-aluminum, and platinum-aluminum were used as trial barrier materials on a $\gamma/\gamma' - \delta$ eutectic alloy. Void formation and diffusion were observed with all of these systems, but W layers showed the least deleterious effects. In practice, unalloyed W would be impractical because of its high susceptibility to oxidation. However, because these basic diffusion studies were done in vacuum, the use of unalloyed W foil was satisfactory.

The objectives of this work were to determine the feasibility of the diffusion barrier concept for coated eutectics, to characterize the specific behavior of a W layer between NiCrAl and $\gamma/\gamma' - \delta$ alloys by using advanced metallographic techniques, and to study the effects of diffusion in directions parallel and perpendicular to the eutectic alloy growth direction.

To more closely relate this work with possible engine hardware, the δ platelet orientations are discussed in terms of the direction of the blade coating and barrier

layers as applied to a turbine component, rather than in terms of the diffusion direction. The orientation of the δ platelets is the same as the growth direction, which is the longitudinal axis of the eutectic alloy bar from which specimens were cut.

Diffusion specimens of eutectic/NiCrAl/W/eutectic were prepared by a hot-press technique and aged in vacuum for as long as 500 hours at 1100^o C. This arrangement * permitted the direct comparison of diffusion at the NiCrAl/substrate interface and at the NiCrAl/W/substrate interfaces. Base-line conditions of element distribution were established by metallographic and electron-beam X-ray microprobe analysis (EMXA) of the as-bonded specimens. The results of this study are presented, and conclusions are drawn from comparisons with the aged specimens.

EXPERIMENTAL PROCEDURES

Materials

The nominal compositions of the γ/γ' - δ eutectic alloys used were (1) Ni - 19.7 wt% Nb - 6.0 wt% Cr - 2.5 wt% Al and (2) Ni - 21.75 wt% Nb - 2.55 wt% Al (ref. 10). The second alloy composition was chosen because it contained no Cr. Thus, Cr could be easily detected if it diffused into the substrate eutectic from the coating. The eutectic alloys were 8 cm long by 1.3 cm in diameter and were obtained from a commercial source. The eutectic alloys were grown in a directional-solidification furnace having a temperature gradient of approximately 300 deg C/cm (ref. 10).

The NiCrAl material had a chemical analysis in weight percent of 19.54 Cr, 3.51 Al, 1.22 Si, 0.7 Fe, 0.4 Mn, 0.03 Co, and 0.076 C and the balance nickel (ref. 4). This alloy with an aluminizing treatment has been shown to provide superior protection to superalloys tested in high-gas-velocity burner rigs at 1090^o C (ref. 11). The material was obtained in the form of 0.66-mm-thick plate.

The W was high purity (99.9 percent) and was obtained as nominally 0.025-mm-thick sheet.

Specimen Preparation

Figure 1 shows a schematic drawing of the diffusion test specimen used in this study and details of the fabrication procedure for preparing test specimens that had the NiCrAl layer perpendicular to the δ platelets. The eutectic alloy bars were first sandblasted to remove external oxide scale; then they were cut into 3.2-mm-thick slices. Disks, 1.3-cm diameter in size, were punched from the NiCrAl plate and the W sheet. Sur-

faces were ground parallel to a 32-rms finish, Zyglo inspected, vapor degreased, ultrasonically cleaned, and then placed in the configuration shown in figure 1.

For test specimens with the NiCrAl layer parallel to the δ platelets (more typical for engine hardware), the eutectic alloy bars were cut in the longitudinal direction, and then into 1.3-cm by 1.3-cm by 0.32-cm slabs. Also 1.3-cm by 1.3-cm slabs were cut from the NiCrAl plate and the W sheet.

The layers were then hot-press bonded at 1100^o C with a pressure of 6.9×10^7 Pa (10 ksi) in a vacuum (total pressure of $<2.7 \times 10^{-3}$ Pa ($<2 \times 10^{-5}$ torr)) for 1 hour. One specimen of each group was cut vertically for metallographic examination of the as-bonded condition and to determine the effectiveness of the bonding process.

Aging Heat Treatments

Specimens were aged for 250 and 500 hours at 1100^o C. All specimens containing 6-wt% Cr in the eutectic alloy were aged in a vertical W-wire-wound tube furnace with a vacuum of 6.7×10^{-2} Pa (5×10^{-4} torr). A temperature controller maintained the temperature in the 7.6-cm isothermal hot zone at $\pm 3^{\circ}$ C. Test temperatures were measured by a Pt/Pt-13Rh thermocouple placed close to the test specimens and were recorded on a strip-chart recorder.

The diffusion specimens with no Cr in the eutectic were encapsulated in quartz under vacuum to avoid any possible Cr pickup from the furnace. The capsules were aged at 1100^o C in a horizontal tube furnace, as described in reference 12.

Metallography

After aging treatments, specimens were sectioned and submitted to metallographic examination and EMXA.

The specimens containing 6-wt% Cr in the eutectic were polished and etched by normal procedures, as specified in reference 13. The final polish was with a 0.5- μ m alumina powder on microcloth. Specimens were etched by immersing them for 5 seconds in a solution of 30 milliliters of nitric acid, 30 milliliters of water, 30 milliliters of acetic acid, and 1 milliliter of hydrofluoric acid.

The specimens containing no Cr in the eutectic were etched with an ion milling apparatus using an argon beam in vacuum, an operating voltage of 7 kV, an ion current of 100 μ A, and a gun current of 2 mA. Ionic etching was necessary because chemical reactions between layers introduced artifacts when attempts were made to chemically etch these specimens.

After standard metallographic examination, the specimens were ultrasonically cleaned and submitted to EMXA analysis. Electrical-conductive tape was placed from the corner of each specimen to the specimen holder. An operating potential of 15 kV and specimen currents of 50 or 100 μ A were used, depending on the current used for the pure comparative standards. Further detailed discussions of the EMXA process are given in references 14 to 16.

EMXA traces were made for the elements Ni, Cr, Al, Nb, and W. The traces were made across the eutectic/NiCrAl interfaces and across the eutectic/W/NiCrAl interfaces of all specimens for comparison of barrier and no-barrier conditions.

Table I summarizes the test conditions and EMXA analyses. It lists the EMXA figures by number and gives the phases traversed. Twenty-four analyses were made with four or five elements each. The EMXA results were computer corrected by the comprehensive COR-2 program (ref. 17) developed by the National Bureau of Standards. This program corrected the raw-intensity EMXA data for background, fluorescence, absorption, backscatter, counter deadtime, and ionization penetration, using an iterative process to develop the final results. Minor elements (<1.5 wt%) were not analyzed but could amount to a maximum of about 2 wt%. An internal check was made on each analysis by summarizing the total weight percent as analyzed. The results were usually well within ± 2 -wt% total of accounting for 100 wt% of the elements present. Final results were normalized to 100 percent for both weight percent and atomic percent of the analyzed elements, and the results were replotted with element weight percent compared with distance from the interfaces. Analytical procedures were the same for as-bonded and aged specimens. The aged specimens and the as-bonded specimens were compared, and the effectiveness of the W barrier was determined.

RESULTS AND DISCUSSION

A great number of parameters have been investigated in this experiment, and much information has been obtained by comprehensive study of the photomicrographs and EMXA results. The following specific topics were selected for detailed analysis: (1) the extent of diffusion between the eutectic alloy and the NiCrAl layer without a barrier layer; (2) the extent of diffusion between the eutectic alloy and the NiCrAl with the W layer, including the interaction of the W with the eutectic and the NiCrAl; and (3) the effect of δ platelet orientation, relative to the NiCrAl and W layers, on the amount of interdiffusion.

Table II presents the diffusion results observed from the EMXA data on the specimen containing 6-wt% Cr in the eutectic alloy for both perpendicular (table II(a)) and parallel (table II(b)) δ platelet orientations. Table III presents the diffusion results

observed on the specimens with no Cr content in the eutectic alloy. Each table lists the as-bonded, 250-hour-aged, and 500-hour-aged data. The phases traversed can be determined by comparing the EMXA figure numbers from table II with the corresponding numbers in table I. The 6-wt% Cr, perpendicularly oriented specimens (table II(a)) are shown in figure 2. These specimens had δ platelet and γ/γ' phases large enough to allow EMXA traces from the NiCrAl into each of the eutectic phases. For the other specimens, tables II(b) and III, a general analysis was run and the phases were identified by reading the intensity ratios of peaks and valleys. The phases of the specimens containing no Cr were too small to be clearly separated by the EMXA analysis.

Photomicrographs of the nine specimen conditions listed in table I are shown in figures 2 to 4, and the EMXA data are reproduced in figures 5 to 7. The photomicrographs and EMXA figures are grouped into three major categories: (1) 6.0-wt% Cr in $\gamma/\gamma' - \delta$, with perpendicular orientation of the platelets to the NiCrAl layer (corresponding to table II(a)); (2) 6.0-wt% Cr in $\gamma/\gamma' - \delta$, with parallel orientation of the platelets to the NiCrAl layer (corresponding to table II(b)); and (3) no Cr content in $\gamma/\gamma' - \delta$, with perpendicular orientation of the platelets to the NiCrAl layer (table III).

Diffusion Between the $\gamma/\gamma' - \delta$ Eutectic Alloy and the NiCrAl Layer

Conclusions are drawn from this research by comparing and analyzing the corresponding photomicrographs and EMXA data for a given interface at aging times of 0, 250, and 500 hours at 1100^o C. For the δ /NiCrAl interface, photomicrographs in figures 2(a), (b), and (c) are compared with the EMXA data presented in figures 5(a), (e), and (i), respectively. The δ platelets were observed to recede to a depth of 30 μm after aging 250 hours at 1100^o C and to a depth of 60 μm after aging 500 hours at 1100^o C. The Nb diffused from the surfaces of the δ phase platelets. It diffused to a depth of 170 μm into the NiCrAl at 250 hours of aging at 1100^o C and to an estimated depth of 250 μm after 500 hours. The portion of the δ phase where Nb had diffused out approached the chemistry of the γ/γ' phases, that is, a combined $\text{Ni}_3(\text{Nb}, \text{Al}, \text{Cr})$ with varying amounts of Nb, Al, and Cr. The sharp interface when the EMXA trace entered the δ phase revealed that the diffusion was clearly surface diffusion from the δ platelets (figs. 5(e) and (i)). No elements were observed to diffuse into the δ platelets. The small gradients indicated in the as-bonded specimens were due to the bonding process and were accentuated by delays in pen recording response and by the relatively large EMXA beam diameter (~1 mm) as it crossed interfaces.

Similarly, in EMXA figures 6(a), (c), and (e), δ recession was also observed to a depth of about 50 μm after 500 hours of aging at 1100^o C, even though this specimen had eutectic platelets parallel to the NiCrAl layer. Niobium diffused approximately 290 μm

into the NiCrAl layer. In the specimens containing no Cr (table III), δ platelet recession was observed to approximately 110 μm and Nb diffusion was observed to approximately 210 μm into the NiCrAl layer (EMXA figs. 7(a), (c), and (e)). In this specimen, as mentioned earlier, the δ phase and the spacings were very small because of the finer structure of the alloy. Separation and accurate analysis of the phases were quite difficult and subjective.

Chromium diffused from the NiCrAl deeply into the γ/γ' phase of the eutectic alloy (table II(a) and EMXA figs. 5(b), (f), and (j)). Chromium decreased in the NiCrAl layer to a depth of 230 μm and also diffused into the eutectic alloy to a depth of about 230 μm after aging for 500 hours at 1100^o C. Similarly, as shown in table III, Cr diffused to about 260 μm into the γ/γ' (EMXA fig. 7(e)). Chromium did not diffuse as deeply into the eutectic when the δ platelets were oriented parallel to the NiCrAl (table II(b) and EMXA fig. 6(e)). This is discussed in more detail in the section on orientation effects.

In summary, the preceding test results show that in all cases without a barrier to diffusion between the NiCrAl and the eutectic, Nb left the δ platelets by surface diffusion and diffused deeply into the NiCrAl. Delta platelets were destroyed at the surface and receded, leaving a phase mixture of $\text{Ni}_3(\text{Nb}, \text{Al}, \text{Cr})$ with varying amounts of Nb, Al, and Cr. The composition is close to that of the γ/γ' phase. No elements were observed to penetrate the remaining δ platelets of the eutectic alloy. Chromium diffused out of the NiCrAl deeply into the γ/γ' phase of the eutectic alloy.

Effect of Tungsten Barrier on Diffusion

When the 0.025-mm-thick layer of W was inserted between the NiCrAl and the eutectic alloy, entirely different diffusion results were obtained. This discussion first focuses on the changes in diffusion brought about by the addition of the W barrier layer and then describes some of the changes in the W barrier layer itself.

From table II(a), the first noticeable effect of the W was that it effectively stopped the δ phase recession. Compare figure 5(k), with barrier, to figure 5(i), no barrier. No Nb was observed to have diffused through the W into the NiCrAl after 500 hours of aging at 1100^o C. Similar results were noted for the parallel orientation (table II(b) and fig. 6(f)). Specimens with no Cr (table III and fig. 7(f)) contained a new phase next to the W barrier on the eutectic side. However, still no Nb was observed to have diffused through the barrier into the NiCrAl after 500 hours of aging.

The W barrier also stopped diffusion of Cr from the NiCrAl into the eutectic alloy. The effect of the Cr diffusion was masked for the 6-wt%-Cr eutectic specimens and the analyses for this element (tables II(a) and (b) and EMXA figs. 5(d), (h), and (l) and 6(b), (d), and (f)) were inconclusive. When the eutectic containing no Cr was tested (table III),

the following results were noted when comparing Cr diffusion with and without the barrier. From EMXA figures 7(d) and (f) and table III, very slight traces of Cr were observed in the γ/γ' after 250 hours and 500 hours, respectively; but these values were very much less than those reported with no barrier - 5 μm as compared with 190 μm at 250 hours, and 70 μm as compared with about 260 μm at 500 hours. The total amounts diffused were much less also (compare EMXA figs. 7(d) and (f) with figs. 7(c) and (e), respectively). Also apparent drops in the Cr content of the NiCrAl layers were observed after aging for 250 and 500 hours with the barrier. The apparent drop in Cr when very little Cr crossed the barrier was probably due to the reduced relative amount of Cr present because extra W had diffused into the same region. Chromium is not believed to be depleting to any significant extent here.

Although very little Cr diffused through the W barrier, the small traces that apparently went into the eutectic are probably the result of the eventual deterioration and limited life of the W barrier. In all aged specimens, the thickness of the W barrier decreased significantly - roughly directly with time. Table II(a) shows that the thickness decreased from an initially measured 30 μm as bonded to 25 μm after 250 hours and to 15 μm after 500 hours of aging. Table II(b) shows thicknesses of 30, 25, and 20 μm at 0, 250, and 500 hours, respectively; and table III shows the same as table II(b). (In all these tables, distances are rounded to the nearest 5 μm . More exact estimates may be made, if desired, by looking at figs. 5 to 7 directly.)

Tungsten has also diffused into the NiCrAl and into the γ/γ' of the eutectic alloy. Table II(a) and figure 5(l) show a W diffusion depth of 60 μm into the γ/γ' and approximately 140 μm into the NiCrAl layer after 500 hours of aging at 1100^o C. From table II(b) and figure 6(f), W has diffused 40 μm into the γ/γ' and about 130 μm into the NiCrAl layer. From table III and figure 7(f), W has diffused 75 μm into the eutectic and about 105 μm into the NiCrAl. Examination of EMXA figure 7(f) revealed W to be high in all the areas adjacent to the W barrier. The phases of the eutectic alloy near the W appear to have been merged or converted into a different phase, $\text{Ni}_3(\text{Nb}, \text{W})$, containing diffusion gradients of W and Nb in which W replaces Nb. In all cases, diffusion was farther into the NiCrAl than into the more complex structured eutectic, probably because the W could only diffuse through the γ/γ' phase of the eutectic.

In summary, these test results show that in all cases the W diffusion barrier between the NiCrAl and the eutectic completely stopped the diffusion of Nb from the δ platelets into the NiCrAl. The δ platelets retained their identity almost to the W barrier, whether they were oriented perpendicular or parallel to the barrier and the NiCrAl. The specimen containing no Cr formed an Nb- and W-rich phase adjacent to the W barriers. The W barrier also greatly reduced the diffusion of Cr from the NiCrAl into the eutectic; only very small traces of Cr were observed in the eutectic alloy after aging. The lifetime of the W barrier appears to be limited and may be re-

lated to its thickness. Tungsten diffused deeply into the NiCrAl and also into the γ/γ' phase of the alloy. Tungsten diffusion was not as deep in the eutectic as in the NiCrAl. This is believed to be due, in part, to the more tortuous path followed as W diffused into the γ/γ' phase.

Silicon was present in the NiCrAl layer at 1.2 wt% in the as-bonded specimen. The silicon was segregated primarily into inclusions in the NiCrAl that tended to increase in size as aging progressed. No significant buildups were noted at any interfaces after aging; and if there were interdiffusion of this element between layers, it was not detected because most readings were so low as to be indistinguishable from the background.

Also, as mentioned earlier, a significant number of voids were observed near the W layer, mostly in the NiCrAl, but some in the eutectic as well. Almost no voids were observed at the $\gamma/\gamma' - \delta - \text{NiCrAl}$ interface in the absence of a W layer. Additional basic work is needed with more elemental materials to observe, identify the cause of, and eliminate this void formation before the diffusion barrier concept can be considered to be feasible for engine application.

Effect of δ Platelet Orientation on Diffusion

Table II(a) presents the results of perpendicular platelet-to-coating orientation and table II(b) presents results of parallel platelet-to-coating orientation. For specimens with no W barrier, after 500 hours of aging at 1100^o C the δ recession was nearly the same for the perpendicular orientation (table II(a) and fig. 5(i)) as for the parallel orientation (table II(b) and fig. 6(e)). However, the diffusion of Cr from the NiCrAl into the γ/γ' phase was approximately 230 μm for the perpendicular orientation (table II(a) and fig. 5(j)) and only 50 μm for the parallel orientation (table II(b) and fig. 6(e)). Niobium in these same studies had diffused from the γ/γ' to a depth of about 160 μm in the perpendicular orientation and only about 50 μm in the parallel orientation (EMXA figs. 5(j) and 6(e)). Niobium appeared to diffuse deeper into the NiCrAl - about 290 μm for the parallel orientation and about 250 μm for the perpendicular orientation. This was probably due to a higher concentration of Nb at the parallel interface. For specimens with W barriers, W diffused into the γ/γ' to a depth of 60 μm when the platelets were perpendicular to the NiCrAl layer and only 40 μm when they were parallel (i. e., ~30 percent less in the parallel direction). All studies supported the conclusion that the parallel orientation of the δ platelets relative to the NiCrAl layer significantly reduced the diffusion of W and Cr into the eutectic alloy as compared with the perpendicular orientation. Fortunately, this parallel orientation is that which would normally be expected for hardware in gas turbine engines.

SUMMARY OF RESULTS

In an effort to determine the feasibility of the diffusion barrier concept, a thin layer of tungsten (W) was placed between a nickel-chromium-aluminum (NiCrAl) layer representing current overlay coatings and a gamma/gamma prime - delta ($\gamma/\gamma' - \delta$) eutectic alloy of the type being considered for turbine blade use. Diffusion couples of eutectic/NiCrAl/W/eutectic were subjected to aging for as long as 500 hours at 1100⁰ C in vacuum. The following results were obtained:

1. With no W barrier, niobium (Nb) left the surfaces of the Ni₃Nb (δ) platelets of the eutectic alloy and diffused into the NiCrAl. The δ platelets thus were destroyed where the Nb had left, and the local composition approached the chemistry of the γ/γ' phase of the eutectic.

2. Also with no barrier, Cr diffused from the NiCrAl deeply into the γ/γ' phase of the eutectic alloy. However, there was no diffusion of Cr into the Ni₃Nb platelets.

3. The W barrier completely stopped the diffusion of Nb from the δ platelets into the NiCrAl.

4. Tungsten greatly reduced the diffusion of Cr from the NiCrAl into the eutectic alloy. Only small traces of Cr diffused through the W after aging.

5. The lifetime of the W barrier appears limited because the thickness decreased with time. Tungsten diffused into the NiCrAl and also into the γ/γ' phase of the eutectic alloy to form a different phase containing diffusion gradients of W and Nb. Also large voids formed in the NiCrAl layer and some formed in the eutectic near the W.

6. After 500 hours of aging at 1100⁰ C, diffusion of elements between the eutectic and the NiCrAl was decreased from 30 percent (W) to 80 percent (Cr), depending on the elements studied, when the NiCrAl layer was parallel to the δ platelets as opposed to being perpendicular to them.

Lewis Research Center,

National Aeronautics and Space Administration,

Cleveland, Ohio, August 31, 1977,

505-01.

REFERENCES

1. Sheffler, K. D.; et al.: Final Report - Alloy and Structural Optimization of a Directionally Solidified Lamellar Eutectic Alloy. (PWA-5300, Pratt & Whitney Aircraft, NASA Contract NAS3-17811.) NASA CR-135000, 1976.

2. Lemkey, F. D.; and McCarthy, G.: Quaternary and Quinary Modifications of Eutectic Superalloys Strengthened by δ , Ni_3Cb Lamellae and γ' , Ni_3Al Precipitates. (UARL-R911698-13, United Aircraft Corp.; NASA Contract NAS3-17785.) NASA CR-134678, 1975.
3. Strangman, T. E.; Felten, E. J.; and Benden, R. S.: Refinement of Promising Coating Compositions for Directionally Cast Eutectics. (PWA-5441, Pratt & Whitney Aircraft; NASA Contract NAS3-18920.) NASA CR-135103, 1976.
4. Gedwill, Michael A.: Cyclic Oxidation Resistance of Clad IN-100 at 1040^o and 1090^o C: Time, Cycle Frequency, and Clad Thickness Effects. NASA TN D-6276, 1971.
5. Veltri, R. D.; Paradis, E. L.; and Douglas, F. C.: Investigation to Develop a Method to Apply Diffusion Barriers to High Strength Fibers. NASA CR-134719, 1975.
6. Douglas, F. C.; Paradis, E. L.; and Veltri, R. D.: Application of Diffusion Barriers to the Refractory Fibers of Tungsten, Columbium, Carbon and Aluminum Oxide. NASA CR-134466, 1973.
7. Rolls, R.; and Shaw, R. D.: The Influence of Borate Coatings on the High-Temperature Oxidation of Iron. Corros. Sci., vol. 14, no. 7, 1974, pp. 431-441.
8. Levinstein, M. A.: Enriched Aluminum Coatings for Dispersion Strengthened Nickel Materials. NASA CR-121250, 1973.
9. Wermuth, F. R.; and Stetson, A. R.: Alloyed Coatings for Dispersion Strengthened Alloys. (RDR-1686-3, Solar Div.; NASA Contract NAS3-14312.) NASA CR-120852, 1971.
10. Lemkey, F. D.: Eutectic Superalloys Strengthened by δ , Ni_3Cb Lamellae and γ' , Ni_3Al Precipitates. NASA CR-2278, 1973.
11. Gedwill, Michael A.; and Grisaffe, Salvatore J.: Oxidation Resistant Claddings for Superalloys. Met. Eng. Q., vol. 12, no. 2, May 1972, pp. 55-61.
12. Levine, Stanley R.: Reaction Diffusion in the Nickel-Chromium-Aluminum and Cobalt-Chromium-Aluminum Systems. NASA TN D-8383, 1977.
13. Tewari, Surendra N.; and Dreshfield, Robert L.: Microstructural Changes Caused by Thermal Treatment and Their Effects on Mechanical Properties of a $\gamma/\gamma' - \delta$ Eutectic Alloy. NASA TN D-8280, 1976.
14. Johnston, James R.; and Young, Stanley G.: Oxidation and Thermal Fatigue of Coated and Uncoated NX-188 Nickel-Base Alloy in a High-Velocity Gas Stream. NASA TN D-6795, 1972.

15. Young, Stanley G.: Microstructural Study of the Nickel-Base Alloy WAZ-20 Using Qualitative and Quantitative Electron Optical Techniques. NASA TN D-7209, 1973.
16. Caves, Robert M.; and Grisaffe, Salvatore J.: Electron and Ion Microprobes Applied to Characterize an Aluminide Coating on IN-100. NASA TN D-6317, 1971.
17. Henoc, Jean; Heinrich, Kurt F. J.; and Myklebust, Robert L.: A Rigorous Correction Procedure for Quantitative Electron Probe Microanalysis (COR-2). NBS-TN-769, Nat. Bur. Stands., 1973.

TABLE I. - SUMMARY OF TEST CONDITIONS AND
EMXA ANALYSES

(a) 6-wt% Cr in $\gamma/\gamma' - \delta$ specimens

Test condition	EMXA figure	Phases traversed
δ Platelets perpendicular to NiCrAl and W layers		
As bonded	5(a)	$\delta \rightarrow \text{NiCrAl}$
	5(b)	$\gamma/\gamma' \rightarrow \text{NiCrAl}$
	5(c)	$\delta \rightarrow \text{W} \rightarrow \text{NiCrAl}$
	5(d)	$\gamma/\gamma' \rightarrow \text{W} \rightarrow \text{NiCrAl}$
250 hr at 1100 ^o C	5(e)	$\delta \rightarrow \text{NiCrAl}$
	5(f)	$\gamma/\gamma' \rightarrow \text{NiCrAl}$
	5(g)	$\delta \rightarrow \text{W} \rightarrow \text{NiCrAl}$
	5(h)	$\gamma/\gamma' \rightarrow \text{W} \rightarrow \text{NiCrAl}$
500 hr at 1100 ^o C	5(i)	$\delta \rightarrow \text{NiCrAl}$
	5(j)	$\gamma/\gamma' \rightarrow \text{NiCrAl}$
	5(k)	$\delta \rightarrow \text{W} \rightarrow \text{NiCrAl}$
	5(l)	$\gamma/\gamma' \rightarrow \text{W} \rightarrow \text{NiCrAl}$
δ Platelets parallel to NiCrAl and W layers		
As bonded	6(a)	$\gamma/\gamma' - \delta \rightarrow \text{NiCrAl}$
	6(b)	$\gamma/\gamma' - \delta \rightarrow \text{W} \rightarrow \text{NiCrAl}$
250 hr at 1100 ^o C	6(c)	$\gamma/\gamma' - \delta \rightarrow \text{NiCrAl}$
	6(d)	$\gamma/\gamma' - \delta \rightarrow \text{W} \rightarrow \text{NiCrAl}$
500 hr at 1100 ^o C	6(e)	$\gamma/\gamma' - \delta \rightarrow \text{NiCrAl}$
	6(f)	$\gamma/\gamma' - \delta \rightarrow \text{W} \rightarrow \text{NiCrAl}$

(b) No Cr in $\gamma/\gamma' - \delta$ specimens; δ platelets perpendicular to NiCrAl and W layers

As bonded	7(a)	$\gamma/\gamma' - \delta \rightarrow \text{NiCrAl}$
	7(b)	$\gamma/\gamma' - \delta \rightarrow \text{W} \rightarrow \text{NiCrAl}$
250 hr at 1100 ^o C	7(c)	$\gamma/\gamma' - \delta \rightarrow \text{NiCrAl}$
	7(d)	$\gamma/\gamma' - \delta \rightarrow \text{W} \rightarrow \text{NiCrAl}$
500 hr at 1100 ^o C	7(e)	$\gamma/\gamma' - \delta \rightarrow \text{NiCrAl}$
	7(f)	$\gamma/\gamma' - \delta \rightarrow \text{W} \rightarrow \text{NiCrAl}$

TABLE II. - APPROXIMATE DEPTHS^a OF SELECTED ELEMENT DIFFUSION BETWEEN LAYERS OF NiCrAl, W, AND $\gamma/\gamma' - \delta$ CONTAINING 6-wt% Cr (FROM EMXA DATA)

(a) δ Platelets perpendicular to NiCrAl and W layers

Specimen condition	EMXA figure	Delta recession	Cr into γ/γ'	Nb from γ/γ'	W into γ/γ'	W thickness	W into NiCrAl	Cr from NiCrAl	Nb into NiCrAl
As bonded	5(a)	5	(c)	(c)	(c)	(c)	(c)	5	20
	5(b)	(c)	5	5	(c)	(c)	(c)	↓	25
	5(c)	0	(c)	(c)	(c)	30	10		0
	5(d)	(c)	0	5	5	30	5		0
250 hr at 1100 ^o C	5(e)	30	(c)	(c)	(c)	(c)	(c)		120
	5(f)	(c)	(130)	(110)	(c)	(c)	(c)	120	(120)
	5(g)	(5)	(c)	(c)	(c)	25	90	(90)	0
	5(h)	(c)	30	30	70	25	90	(90)	0
500 hr at 1100 ^o C	5(i)	60	(c)	(c)	(c)	(c)	(c)	230	(250)
	5(j)	(c)	(230)	(160)	(c)	(c)	(c)	230	(200)
	5(k)	5	(c)	(c)	(c)	15	(140)	(90)	0
	5(l)	(c)	30	30	60	15	(140)	(90)	0

(b) δ Platelets parallel to NiCrAl and W layers

As bonded	6(a)	(5)	5	(5)	(c)	(c)	(c)	5	15
	6(b)	0	0	5	5	30	10	5	0
250 hr at 1100 ^o C	6(c)	(35)	(40)	(35)	(c)	(c)	(c)	(150)	200
	6(d)	0	5	(15)	20	25	(120)	(60)	0
500 hr at 1100 ^o C	6(e)	(50)	(50)	(50)	(c)	(c)	(c)	(170)	(290)
	6(f)	0	5	(15)	40	20	(130)	(90)	0

^aDistances are measured in micrometers to the nearest 5 μm from the $(\gamma/\gamma' - \delta)/\text{NiCrAl}$ interface, the $(\gamma/\gamma' - \delta)/\text{W}$ interface, or the W/NiCrAl interface, whichever is applicable. Nickel and aluminum are not reported here because similar levels of these elements on both sides of the interfaces and variations within two- or three-phase regions make determination of the extent of diffusion nearly impossible or, at least, very subjective.

^bParentheses denote extrapolated and/or estimated values.

^cNot applicable.

TABLE III. - APPROXIMATE DEPTHS^a OF SELECTED ELEMENT DIFFUSION BETWEEN LAYERS OF NiCrAl, W, AND $\gamma/\gamma' - \delta$ CONTAINING NO CR (FROM EMXA DATA)

[δ Platelets perpendicular to NiCrAl and W layers.]

Specimen condition	EMXA figure	Delta recession	Cr into γ/γ'	Nb from γ/γ'	W into γ/γ'	W thickness	W into NiCrAl	Cr from NiCrAl	Nb into NiCrAl
As bonded	7 (a)	5	5	5	(c)	(c)	(c)	5	10
	7 (b)	0	0	0	5	30	5	^d 5	0
250 hr at 1100 ^o C	7 (c)	(60)	(190)	(90)	(c)	(c)	(c)	(120)	(190)
	7 (d)	^e (30)	^e 5	^d (30)	75	25	80	^d 60	0
500 hr at 1100 ^o C	7 (e)	(110)	(260)	(110)	(c)	(c)	(c)	(180)	(210)
	7 (f)	^e (40)	^f 70	^e (40)	70	20	105	^d 95	0

^aDistances are measured in micrometers to the nearest 5 μm from the $(\gamma/\gamma' - \delta)/\text{NiCrAl}$ interface, the $(\gamma/\gamma' - \delta)/\text{W}$ interface, or the W/NiCrAl interface, whichever is applicable. Nickel and aluminum are not reported here because similar levels of these elements on both sides of the interfaces and variations within two- to three-phase regions make determination of the extent of diffusion very subjective.

^bParentheses denote extrapolated and/or estimated values.

^cNot applicable.

^dThe apparent drop in Cr when very little Cr diffuses across the W barrier is probably due to the reduced relative amount of Cr from the extra W that has diffused into the same area. Cr is not believed to be depleting in this region.

^eThis value represents the thickness of a new phase, next to the W barrier, which has nearly constant Ni and Al, with diffusion gradients of Nb and W.

^fA trace detected, usually much less than 0.5 wt%.

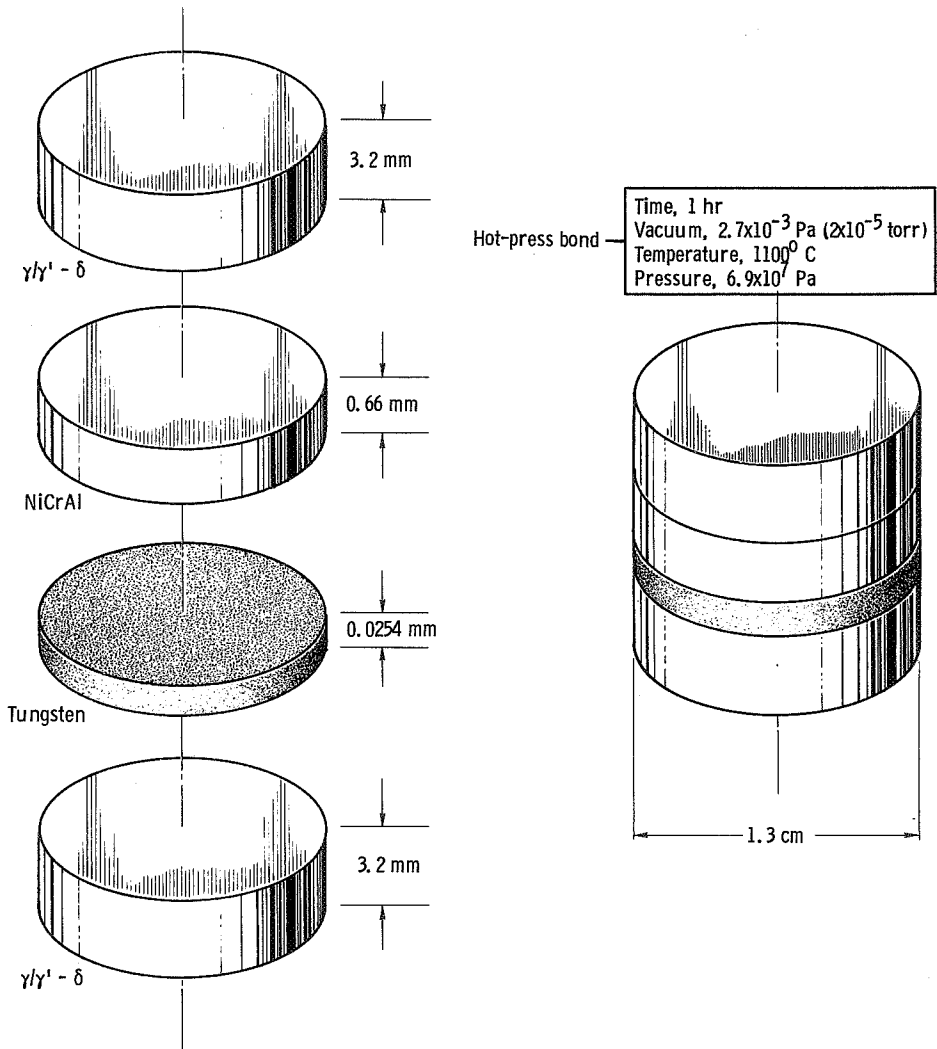
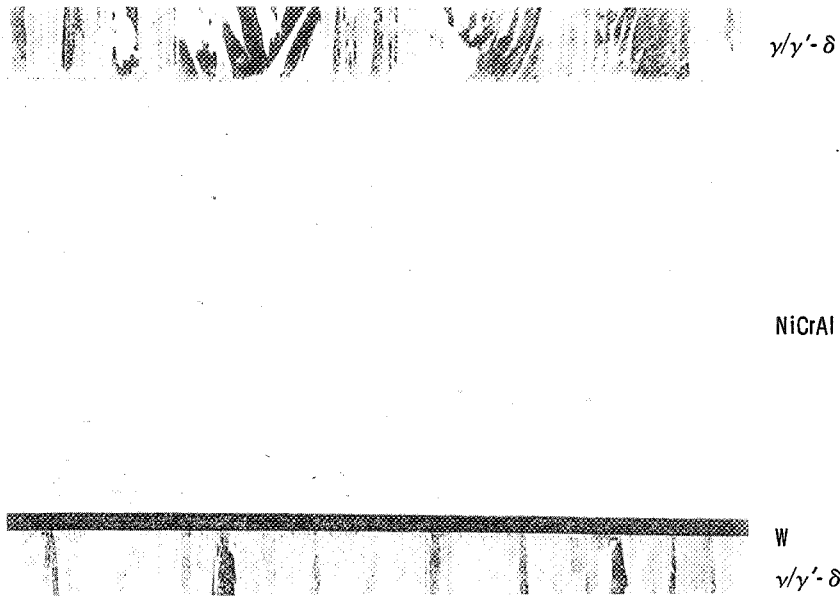


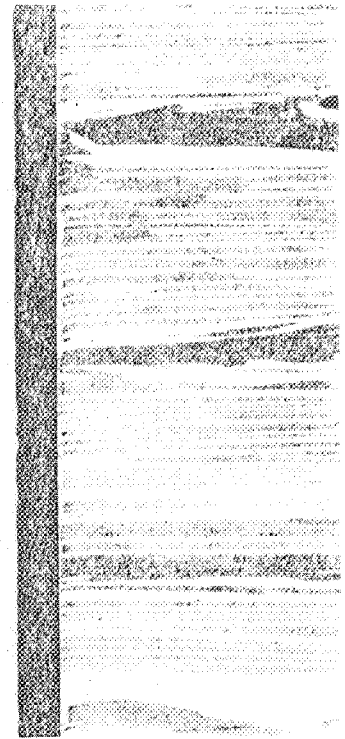
Figure 1. - Diffusion test specimen of $(\gamma/\gamma' - \delta)/\text{NiCrAl}/\text{W}/(\gamma/\gamma' - \delta)$.



(a-1) Overview showing all interfaces. X100.



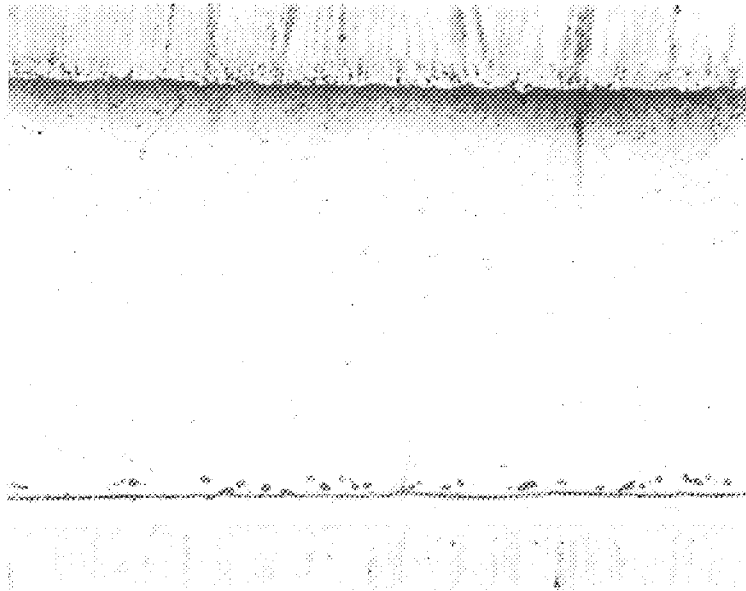
(a-2) $(\gamma/\gamma'-\delta)/\text{NiCrAl}$ interface. X250.



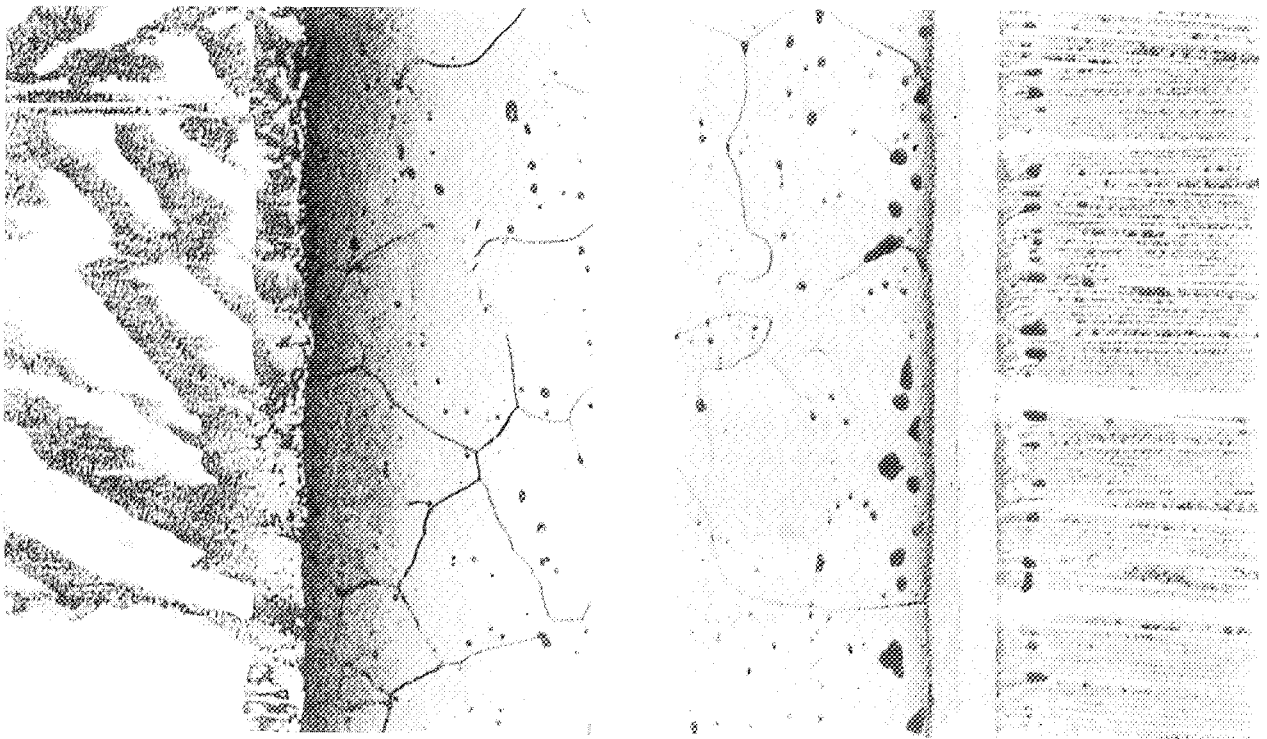
(a-3) $\text{NiCrAl}/\text{W}/(\gamma/\gamma'-\delta)$ interfaces. X250.

(a) As hot-press bonded.

Figure 2. - Diffusion specimens of $(\gamma/\gamma'-\delta)/\text{NiCrAl}/\text{W}/(\gamma/\gamma'-\delta)$. δ Platelets oriented perpendicular to NiCrAl and to W barrier; Cr content in $\gamma/\gamma'-\delta$, 6 wt %.



(b-1) Overview showing all interfaces. X100.

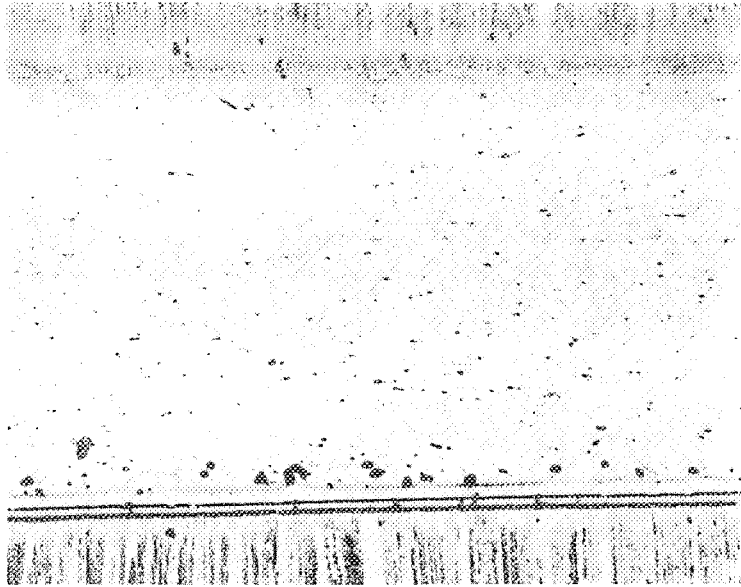


(b-2) $(\gamma/\gamma' - \delta)/\text{NiCrAl}$ interface. X250.

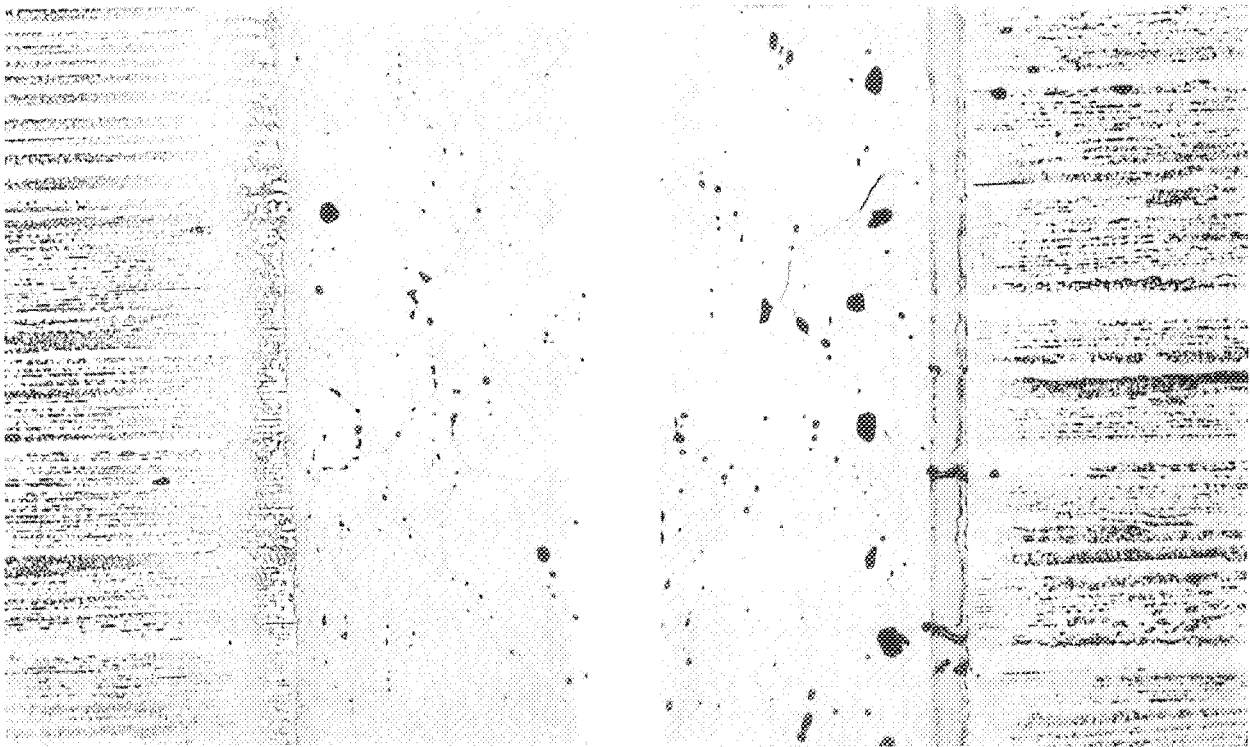
(b-3) $\text{NiCrAl}/\text{W}/(\gamma/\gamma' - \delta)$ interfaces. X250.

(b) Aged 250 hours at 1100° C.

Figure 2. - Continued.



(c-1) Overview showing all interfaces. X100.

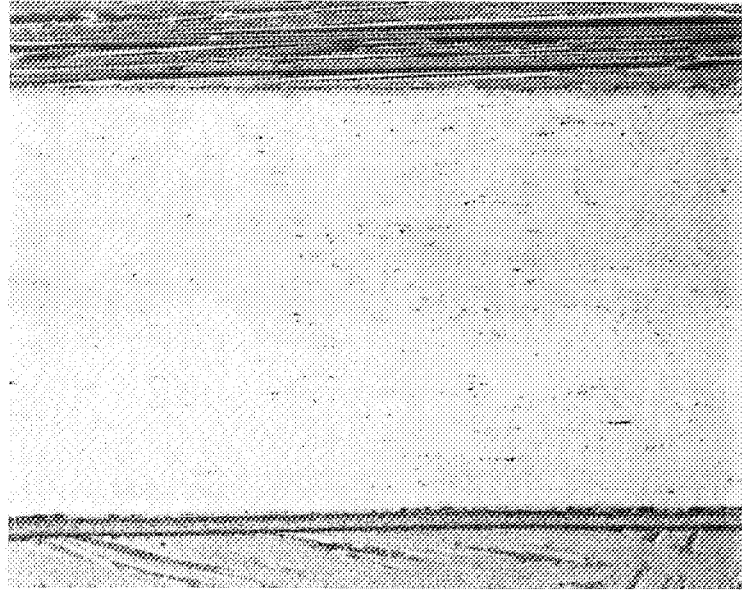


(c-2) $(\gamma/\gamma' - \delta)/\text{NiCrAl}$ interface. X250.

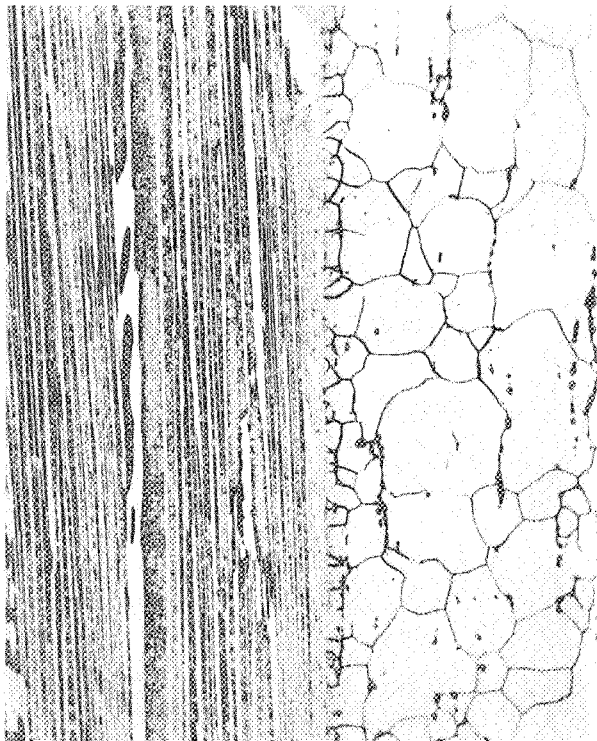
(c-3) NiCrAl/W/ $(\gamma/\gamma' - \delta)$ interfaces. X250.

(c) Aged 500 hours at 1100° C.

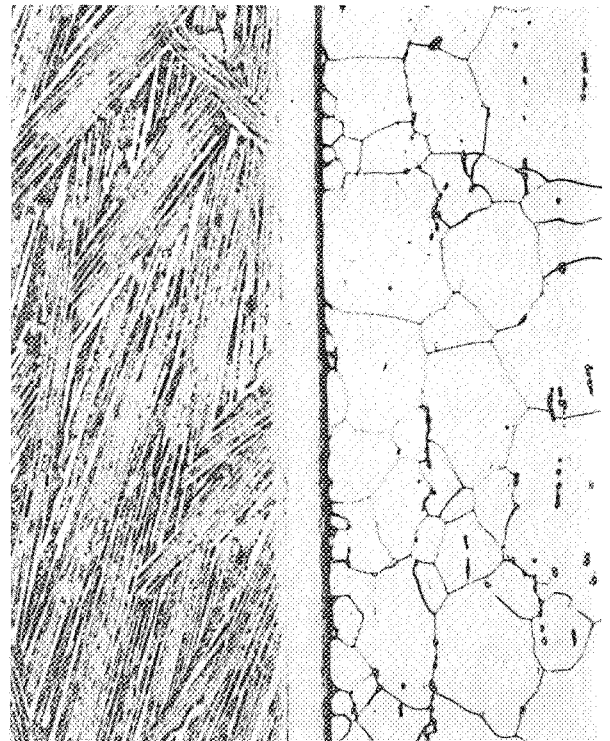
Figure 2. - Concluded.



(a-1) Overview showing all interfaces. X100.



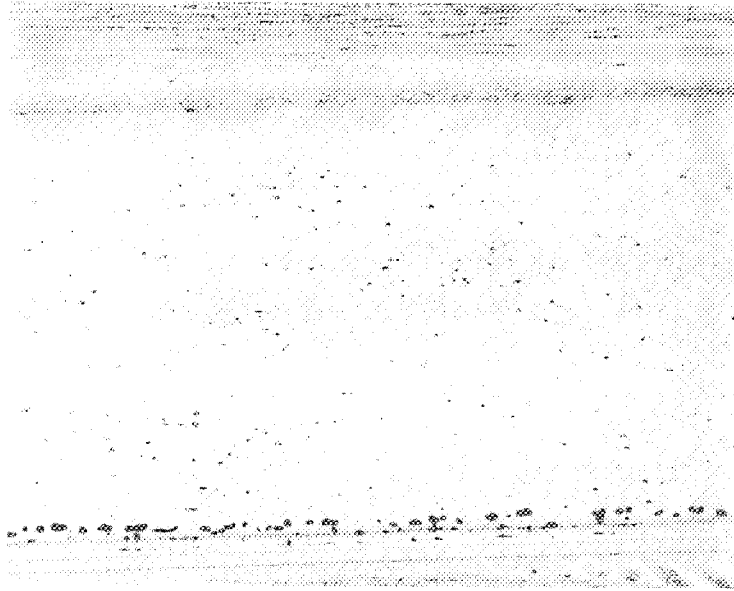
(a-2) $(\gamma/\gamma'-\delta)/\text{NiCrAl}$ interface. X250.



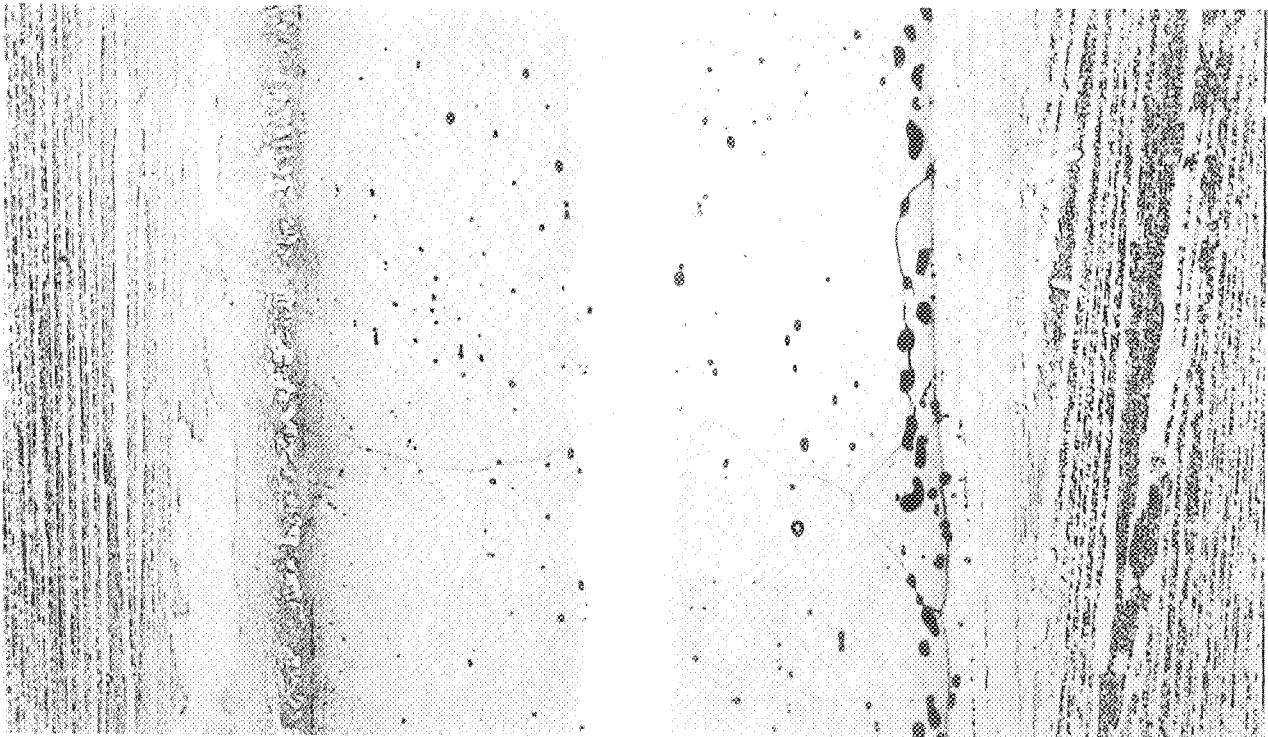
(a-3) $\text{NiCrAl}/\text{W}/(\gamma/\gamma'-\delta)$ interfaces. X250.

(a) As hot-press bonded.

Figure 3. - Diffusion specimens of $(\gamma/\gamma'-\delta)/\text{NiCrAl}/\text{W}/(\gamma/\gamma'-\delta)$. δ Platelets oriented parallel to NiCrAl and to W barrier; Cr content in $\gamma/\gamma'-\delta$, 6 wt %.



(b-1) Overview showing all interfaces. X100.

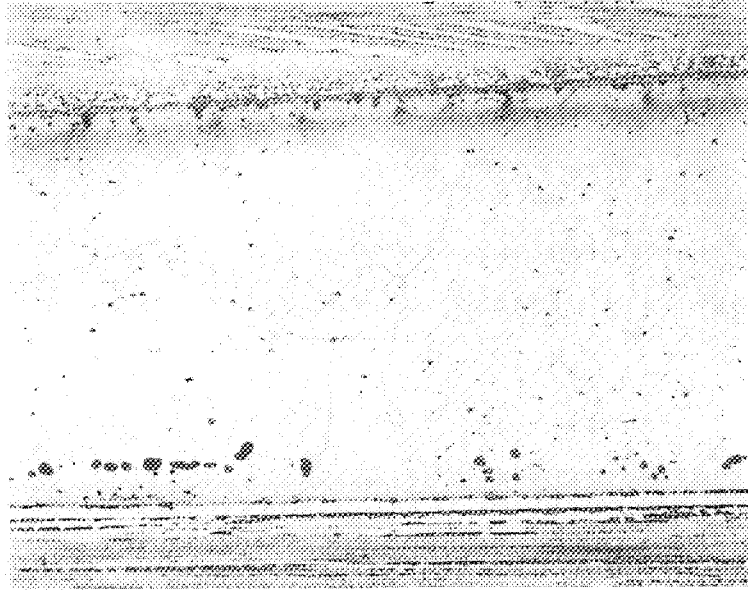


(b-2) $(\gamma/\gamma'-\delta)/\text{NiCrAl}$ interface. X250.

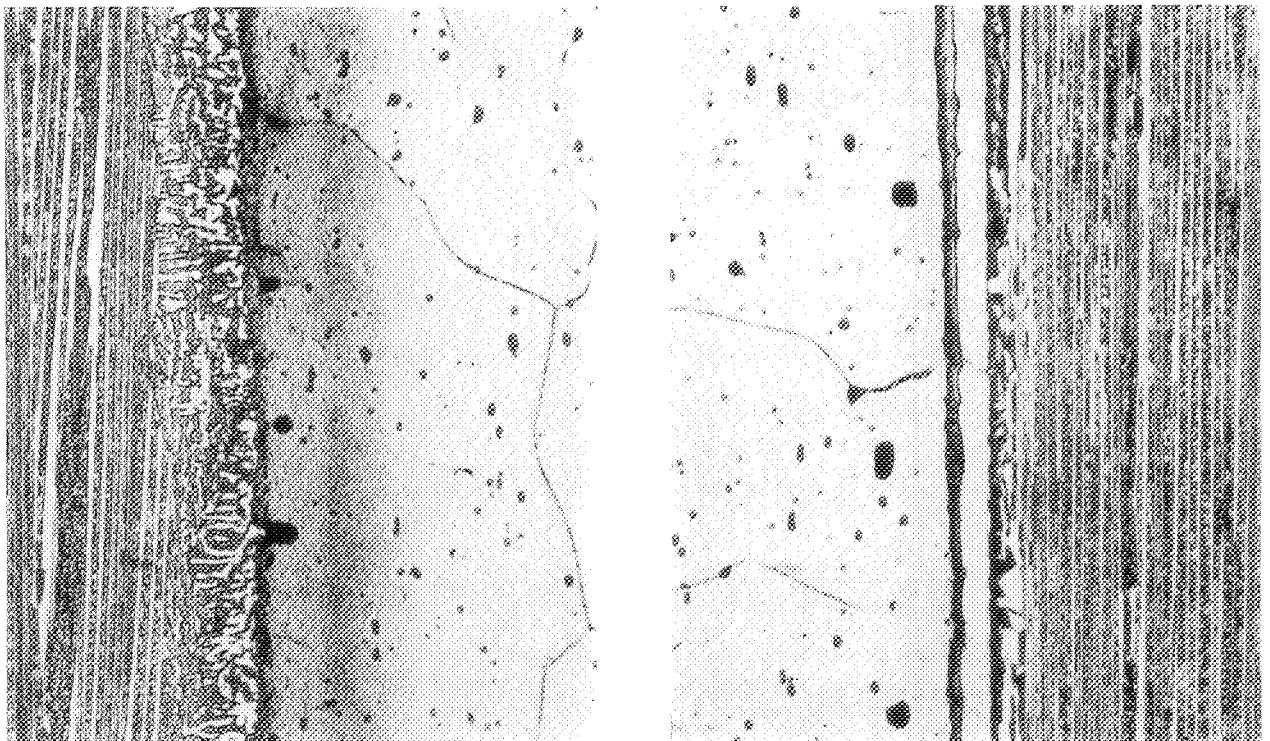
(b-3) $\text{NiCrAl/W}/(\gamma/\gamma'-\delta)$ interfaces. X250.

(b) Aged 250 hours at 1100°C.

Figure 3. - Continued.



(c-1) Overview showing all interfaces. X100.



(c-2) $(\gamma/\gamma' - \delta)$ /NiCrAl interface. X250.

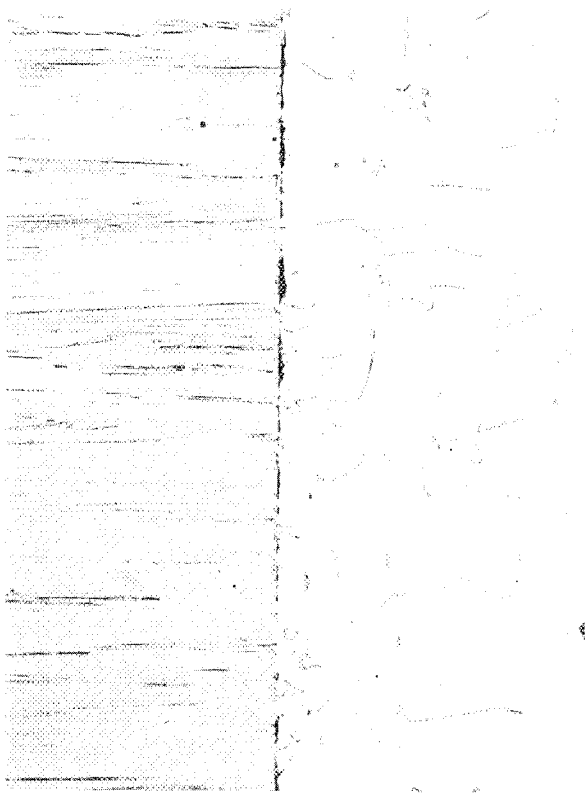
(c-3) NiCrAl/W/ $(\gamma/\gamma' - \delta)$ interfaces. X250.

(c) Aged 500 hours at 1100° C.

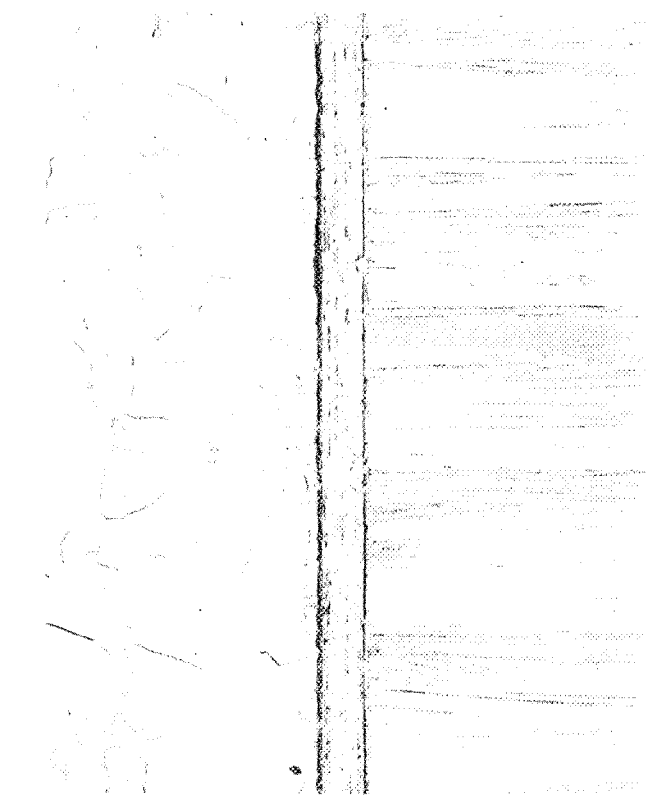
Figure 3. - Concluded.



(a-1) Overview showing all interfaces. X100.



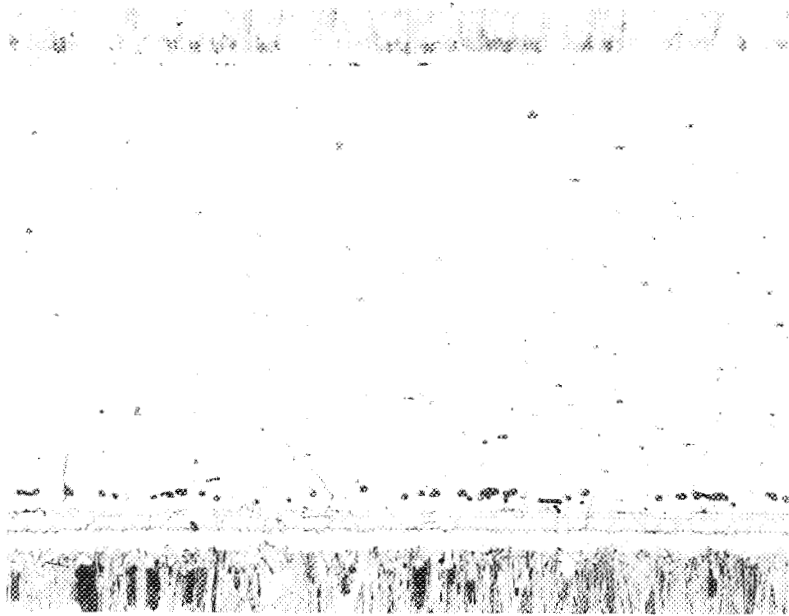
(a-2) $(\gamma/\gamma'-\delta)/\text{NiCrAl}$ interface. X250.



(a-3) $\text{NiCrAl}/\text{W}/(\gamma/\gamma'-\delta)$ interfaces. X250.

(a) As hot-press bonded.

Figure 4. - Diffusion specimens of $(\gamma/\gamma'-\delta)/\text{NiCrAl}/\text{W}/(\gamma/\gamma'-\delta)$. δ Platelets oriented perpendicular to NiCrAl and to W barrier; Cr content in $\gamma/\gamma'-\delta$, 0.



(b-1) Overview showing all interfaces. X100.

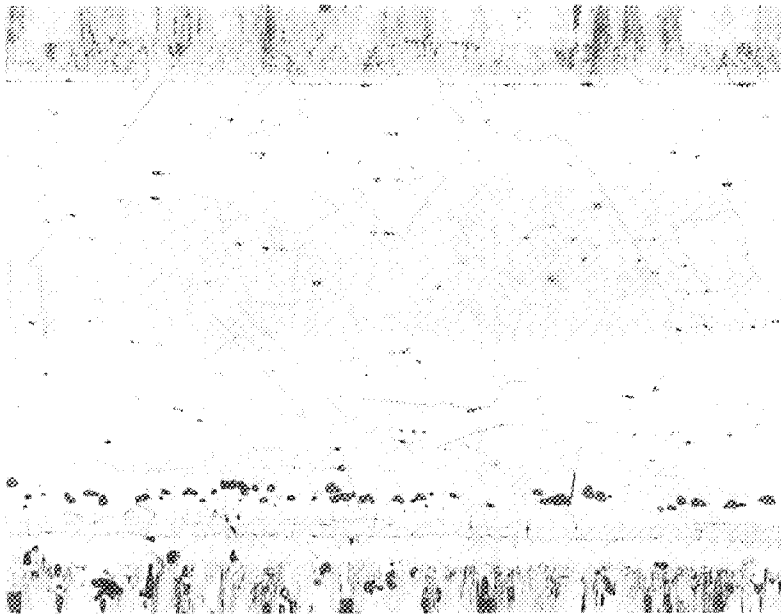


(b-2) $(\gamma/\gamma' - \delta)$ /NiCrAl interface. X250.

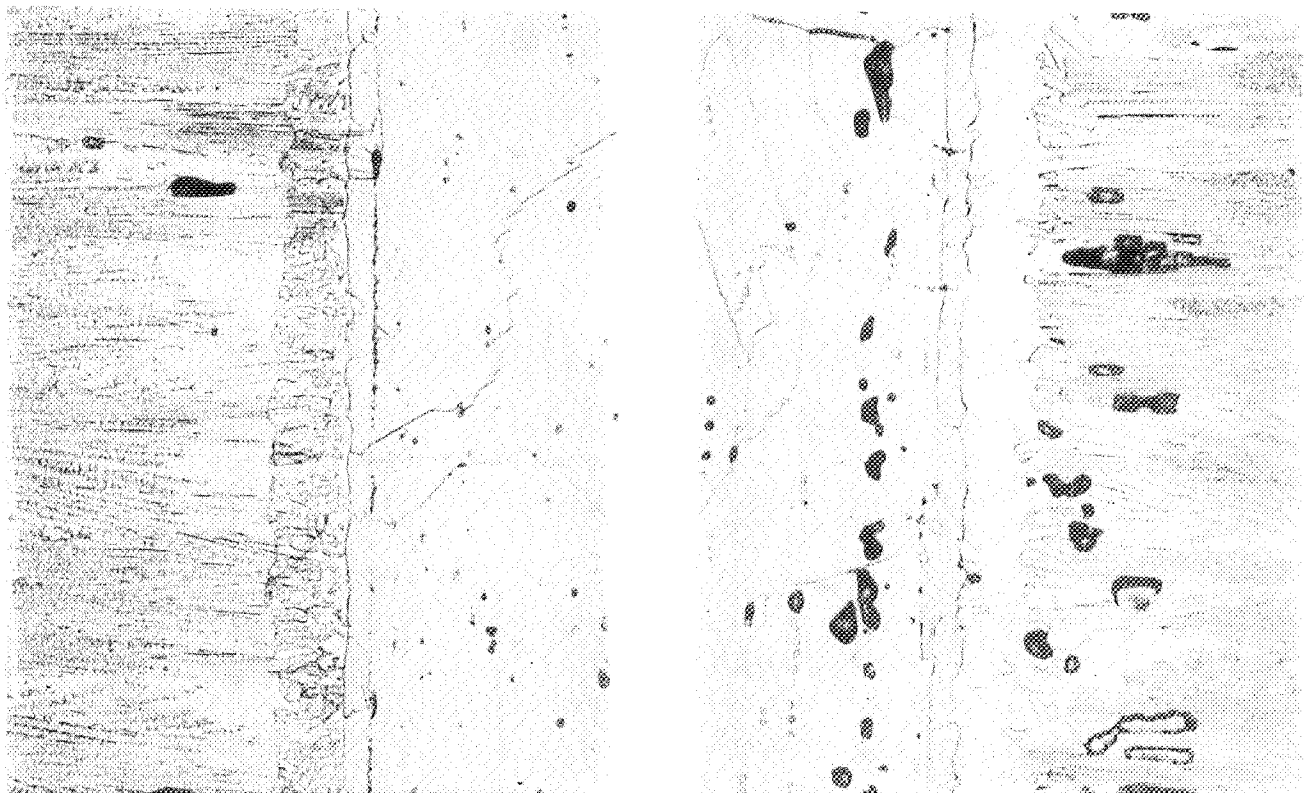
(b-3) NiCrAl/W/ $(\gamma/\gamma' - \delta)$ interfaces. X250.

(b) Aged 250 hours at 1100° C.

Figure 4. - Continued.



(c-1) Overview showing all interfaces. X100.



(c-2) $(\gamma/\gamma'-\delta)/\text{NiCrAl}$ interface. X250.

(c-3) $\text{NiCrAl}/\text{W}/(\gamma/\gamma'-\delta)$ interfaces. X250.

(c) Aged 500 hours at 1100°C.

Figure 4. - Concluded.

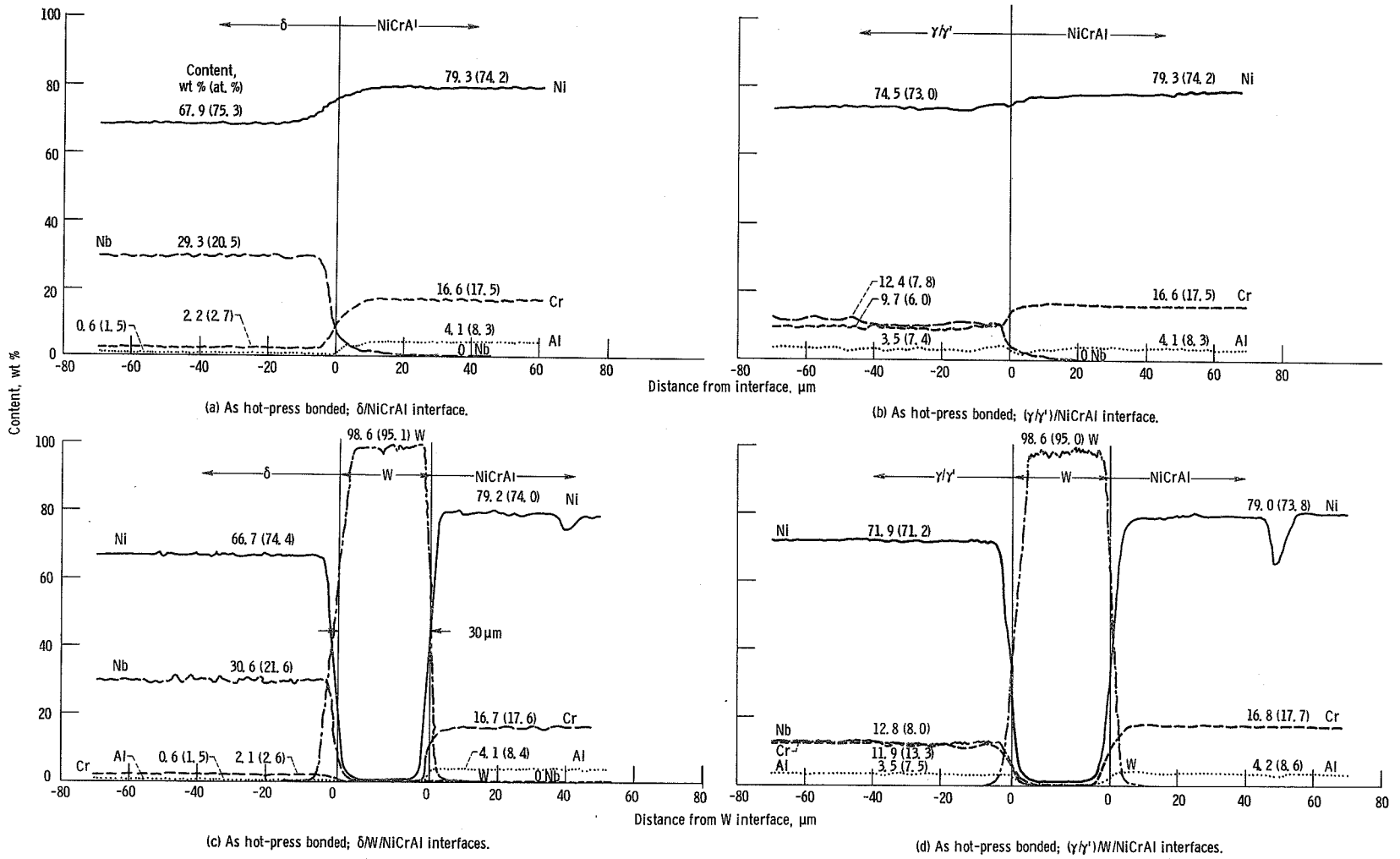
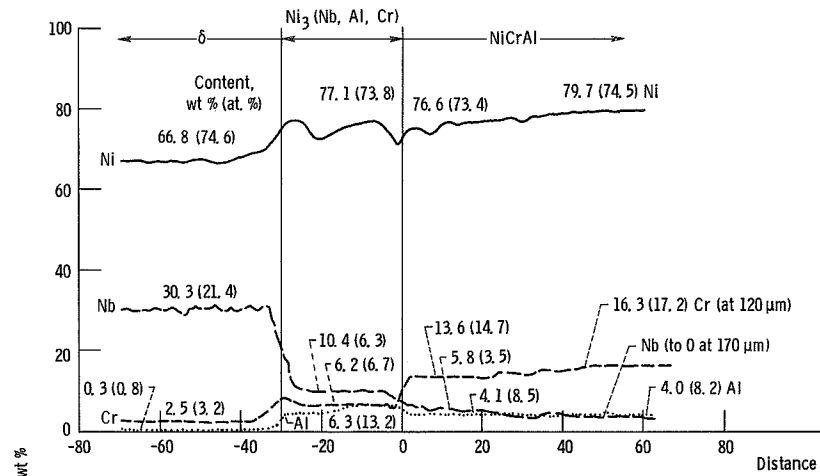
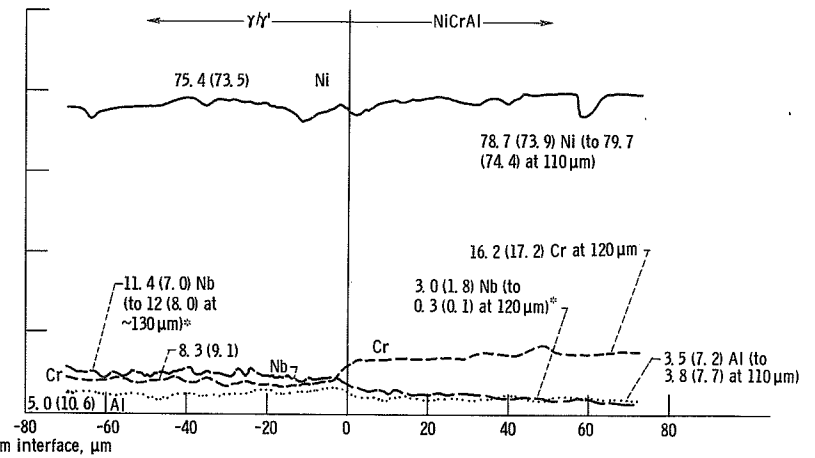


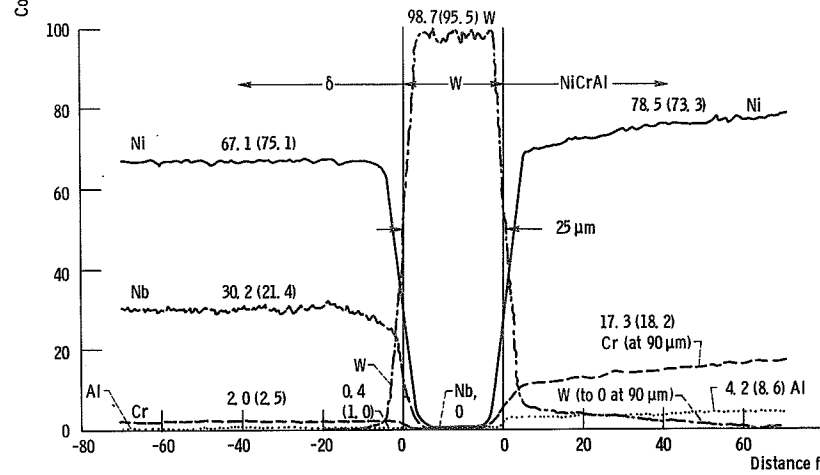
Figure 5. - Electron-microprobe X-ray analysis (EMXA) traces across diffusion specimens of $(\gamma/\gamma' - \delta)$ /NiCrAl/ $(\gamma/\gamma' - \delta)$. δ Platelets oriented perpendicular to NiCrAl and to W barrier; Cr content in $\gamma/\gamma' - \delta$, 6 wt %



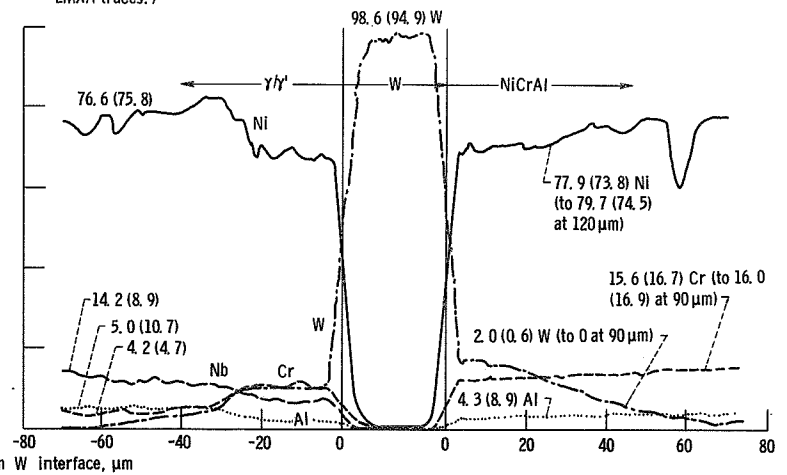
(e) Aged 250 hours at 1100^o C; δ /NiCrAl interface.



(f) Aged 250 hours at 1100^o C; γ/γ' /NiCrAl interface. (*Numbers estimated or extrapolated on original EMXA traces.)



(g) Aged 250 hours at 1100^o C; δ /W/NiCrAl interfaces.



(h) Aged 250 hours at 1100^o C; γ/γ' /W/NiCrAl interfaces.

Figure 5. - Continued.

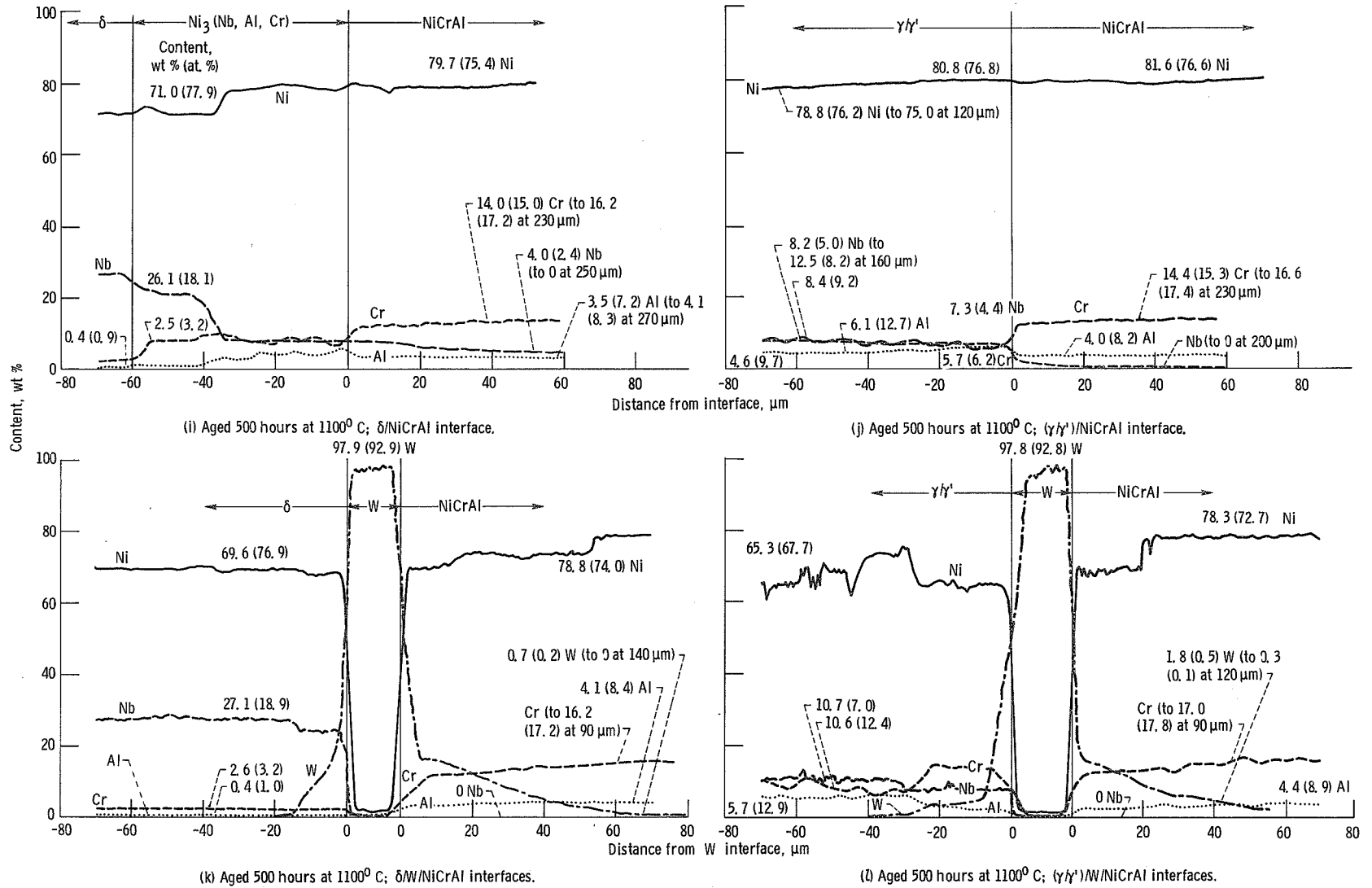
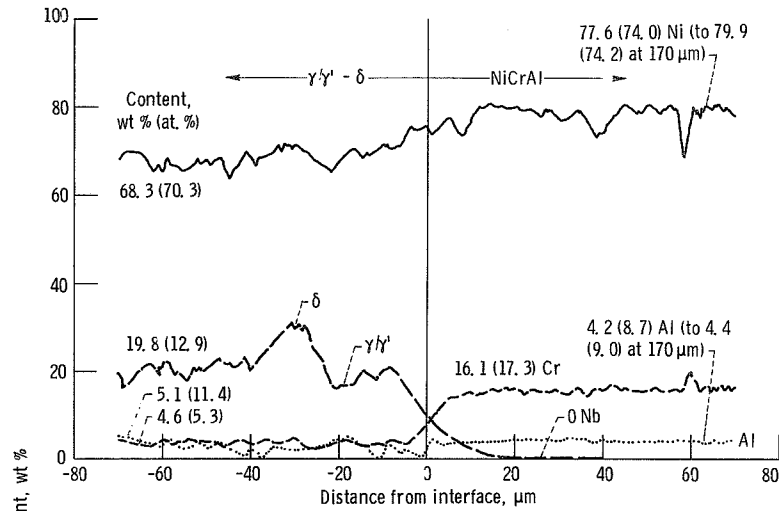
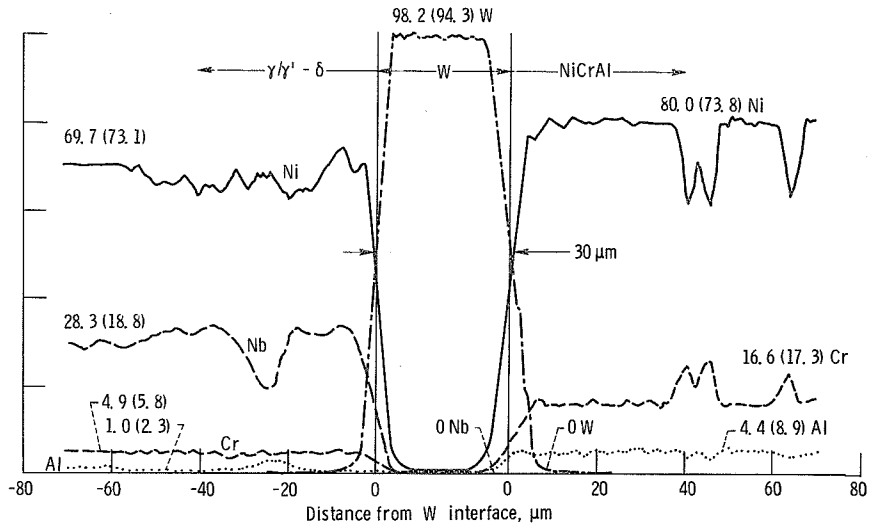


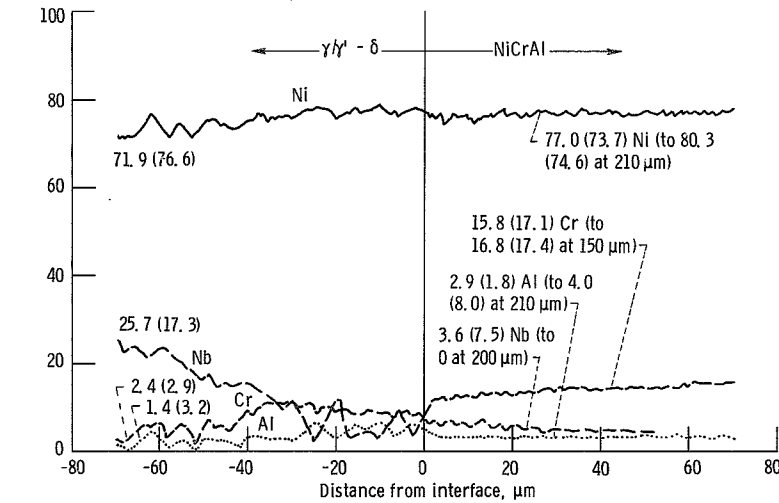
Figure 5. - Concluded.



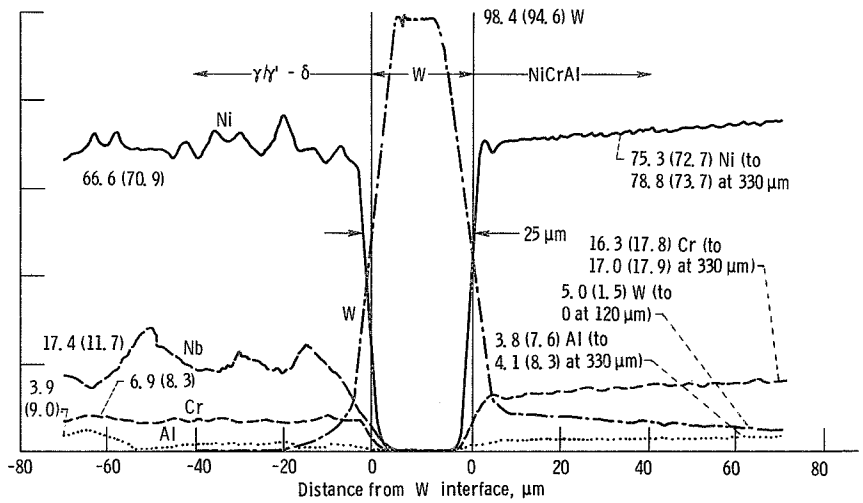
(a) As hot-press bonded; $(\gamma/\gamma' - \delta)/\text{NiCrAl}$ interface.



(b) As hot-press bonded; $(\gamma/\gamma' - \delta)/\text{W}/\text{NiCrAl}$ interfaces.

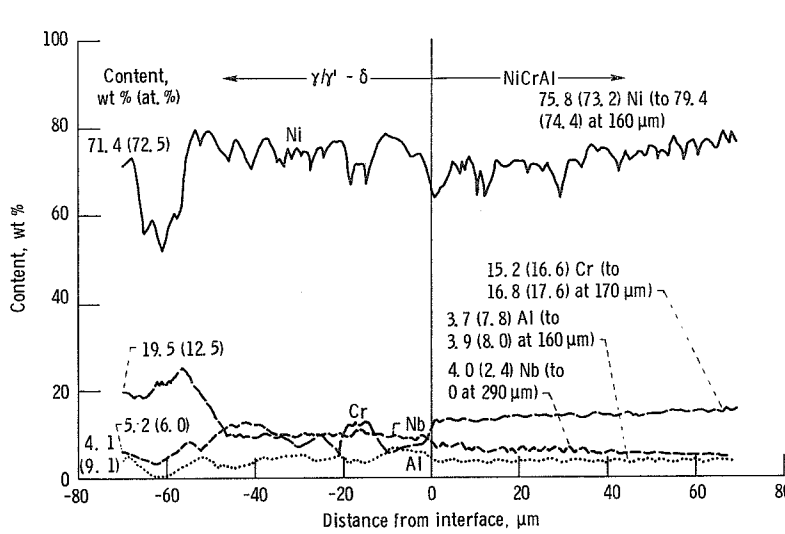


(c) Aged 250 hours at 1100°C ; $(\gamma/\gamma' - \delta)/\text{NiCrAl}$ interface.

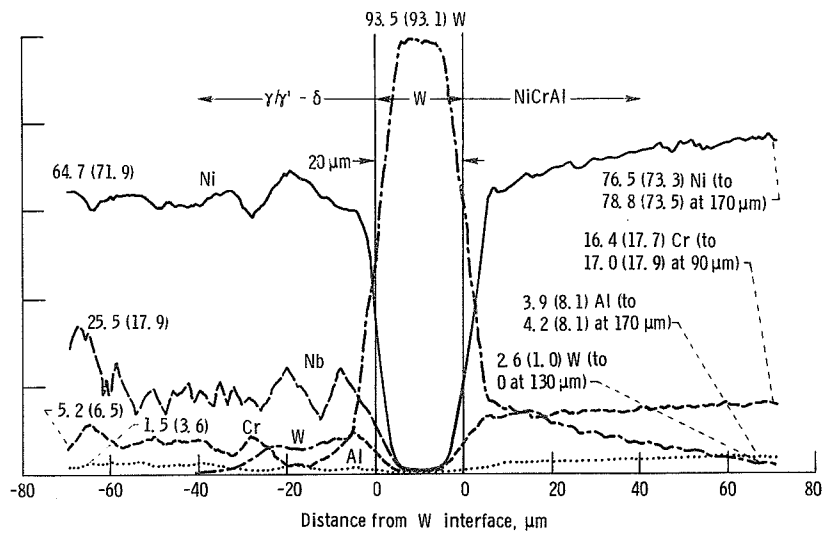


(d) Aged 250 hours at 1100°C ; $(\gamma/\gamma' - \delta)/\text{W}/\text{NiCrAl}$ interfaces.

Figure 6. - Electron-microprobe X-ray analysis (EMXA) traces across diffusion specimens of $(\gamma/\gamma' - \delta)/\text{NiCrAl}/\text{W}/(\gamma/\gamma' - \delta)$. δ Platelets oriented parallel to NiCrAl and W barrier; Cr content in $\gamma/\gamma' - \delta$, 6 wt %.

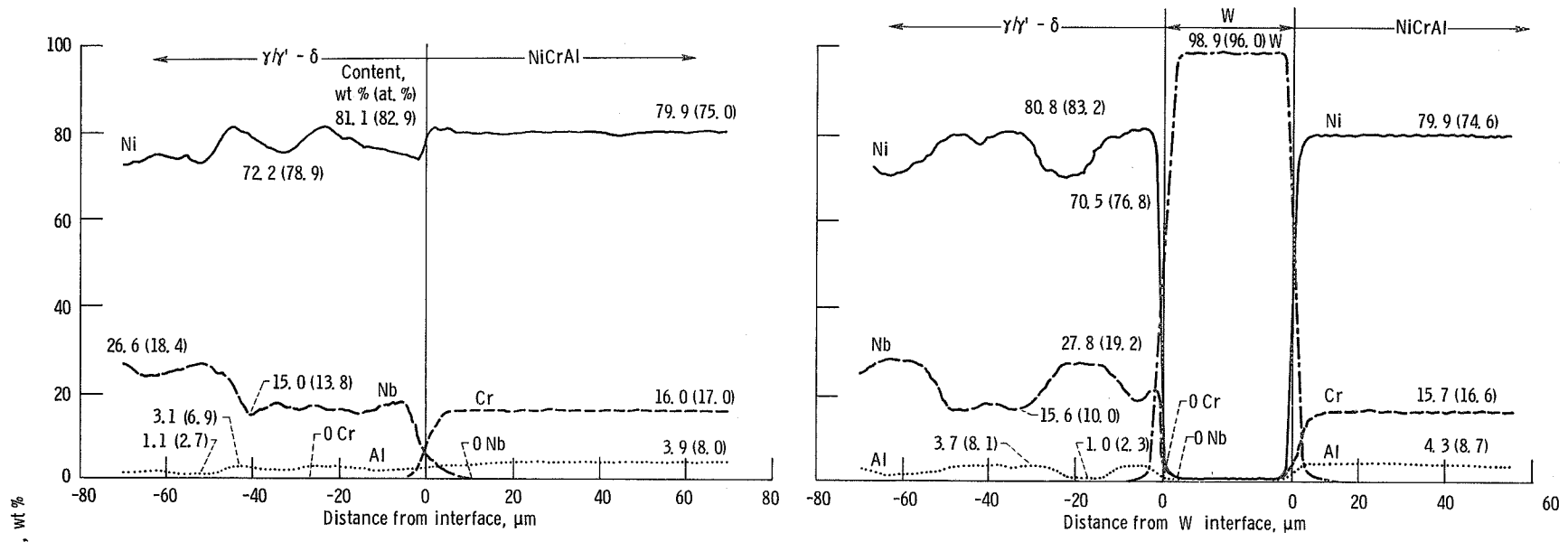


(e) Aged 500 hours at 1100^o C; ($\gamma/\gamma' - \delta$)/NiCrAl interface.



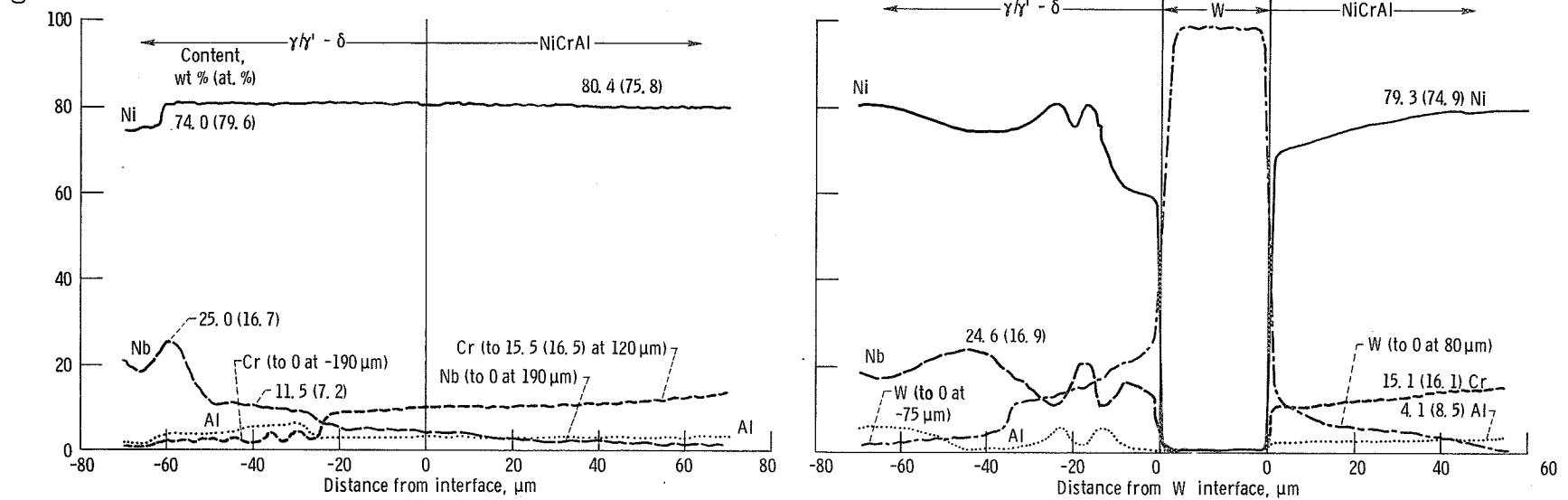
(f) Aged 500 hours at 1100^o C; ($\gamma/\gamma' - \delta$)/W/NiCrAl interfaces.

Figure 6. - Concluded.



(a) As hot-press bonded; $(\gamma/\gamma' - \delta)/\text{NiCrAl}$ interface.

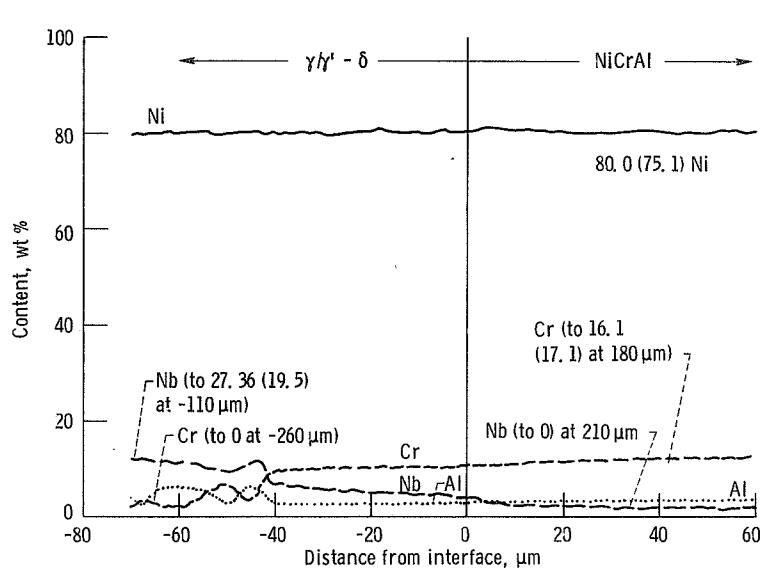
(b) As hot-press bonded; $(\gamma/\gamma' - \delta)/\text{W}/\text{NiCrAl}$ interfaces.



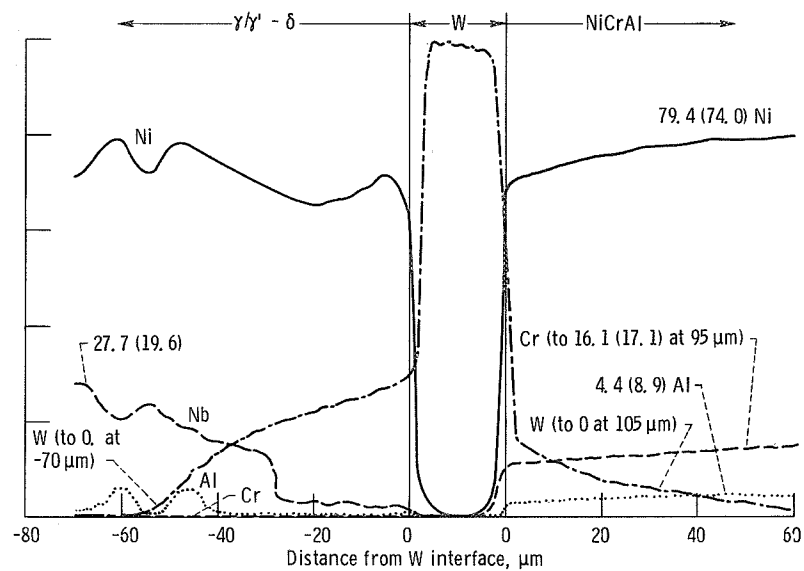
(c) Aged 250 hours at 1100°C ; $(\gamma/\gamma' - \delta)/\text{NiCrAl}$ interface.

(d) Aged 250 hours at 1100°C ; $(\gamma/\gamma' - \delta)/\text{W}/\text{NiCrAl}$ interfaces.

Figure 7. - Electron-microprobe X-ray analysis (EMXA) traces across diffusion specimens of $(\gamma/\gamma' - \delta)/\text{NiCrAl}/(\gamma/\gamma' - \delta)$. δ Platelets oriented perpendicular to NiCrAl and to W barrier; Cr content in $\gamma/\gamma' - \delta$, 0.



(e) Aged 500 hours at 1100^o C; ($\gamma/\gamma' - \delta$)/NiCrAl interface.



(f) Aged 500 hours at 1100^o C; ($\gamma/\gamma' - \delta$)/W/NiCrAl interfaces.

Figure 7. - Concluded.

1. Report No. NASA TP-1131	2. Government Accession No.	3. Recipient's Catalog No.	
4. Title and Subtitle FEASIBILITY STUDY OF TUNGSTEN AS A DIFFUSION BARRIER BETWEEN NICKEL-CHROMIUM-ALUMINUM AND γ/γ' - δ EUTECTIC ALLOYS		5. Report Date January 1978	6. Performing Organization Code
		8. Performing Organization Report No. E-9271	10. Work Unit No. 505-01
7. Author(s) Stanley G. Young and Glenn R. Zellars		11. Contract or Grant No.	
9. Performing Organization Name and Address National Aeronautics and Space Administration Lewis Research Center Cleveland, Ohio 44135		13. Type of Report and Period Covered Technical Paper	
		14. Sponsoring Agency Code	
12. Sponsoring Agency Name and Address National Aeronautics and Space Administration Washington, D.C. 20546		15. Supplementary Notes	
16. Abstract Coating systems have been proposed for potential use on eutectic alloy components in high-temperature gas turbine engines. In a study to prevent deterioration of such systems by diffusion, a 25- μ m (1-mil) thick W sheet was placed between eutectic alloys and a NiCrAl layer. Layered test specimens were aged at 1100 ^o C for as long as 500 hours. Without the W barrier, the delta phase of the eutectic deteriorated by diffusion of Nb into the NiCrAl. Insertion of the W barrier stopped the diffusion of Nb from δ . Chromium diffusion from the NiCrAl into the γ/γ' phase of the eutectic was greatly reduced by the barrier. However, the barrier thickness decreased with time; and W diffused into both the NiCrAl and the eutectic. When the δ platelets were alined parallel to the NiCrAl layer, rather than perpendicular, diffusion into the eutectic was reduced.			
17. Key Words (Suggested by Author(s)) Diffusion; Diffusion barrier; Barrier layers; Coatings; Gas-turbine engine materials; Eutectic alloys; NiCrAl; Tungsten; High-temperature materials		18. Distribution Statement Unclassified - unlimited STAR Category 26	
19. Security Classif. (of this report) Unclassified	20. Security Classif. (of this page) Unclassified	21. No. of Pages 33	22. Price* A03

* For sale by the National Technical Information Service, Springfield, Virginia 22161